T.C.
VAN YÜZÜNCÜ YIL UNIVERSITY
HEALTH SCINECES INSTITUTE

# INVESTIGATION OF WOUND HEALING EFFECT OF HYALURONIC ACID/PULLULAN GEL FORMULATIONS

Saad Khalaf Matloob ALMATLOB
BASIC PHARMACEUTICAL SCIENCES
(PHARMACY PROGRAMME)
MASTER SCIENCE THESIS

ADVISORS
Asst. Prof. Dr. Ömer TÜRKMEN
Assoc. Prof. Dr. Mert İLHAN

VAN-2024

T.C.
VAN YÜZÜNCÜ YIL UNIVERSITY
HEALTH SCIENCE INSTITUTE

# INVESTIGATION OF WOUND HEALING EFFECT OF HYALURONIC ACID/PULLULAN GEL FORMULATIONS

Saad Khalaf Matloob ALMATLOB
BASIC PHARMACEUTICAL SCIENCES
(PHARMACY PROGRAMME)
MASTER SCIENCE THESIS

ADVISORS
Asst. Prof. Dr. Ömer TÜRKMEN
Assoc. Prof. Dr. Mert İLHAN

VAN-2024

This thesis was supported by VAN YYU Scinetific Research Projects Department (Project Number TYL-2022-10063)

T.C.
VAN YÜZÜNCÜ YIL ÜNİVERSİTESİ
SAĞLIK BİLİMLERİ ENSTİTÜSÜ

**KABUL VE ONAY**

Van Yüzüncü Yıl Üniversitesi Sağlık Bilimleri Enstitüsü, Temel Eczacılık Bilimleri Anabilim Dalı'nda Saad Khalaf Matloob ALMATLOB tarafından hazırlanan "*Investigation of Wound Healing Effect of Hyaluronic Acid/Pullulan Gel Formulations"* adlı tez çalışması aşağıdaki jüri tarafından YÜKSEK LİSANS TEZİ olarak OY BİRLİĞİ ile kabul edilmiştir.

Tez Savunma Tarihi: 26/12/2023

Doç. Dr. Mehmet BERKÖZ
Van Yüzüncü Yıl Üniversitesi
Jüri Başkanı

Dr. Öğr. Üyesi Ömer TÜRKMEN
Van Yüzüncü Yıl Üniversitesi
Jüri Üyesi

Doç. Dr. Oruç YUNUSOĞLU
Bolu Abant İzzet Baysal Üniversitesi
Jüri Üyesi

Tez hakkında alınan jüri kararı, Van Yüzüncü Yıl Üniversitesi Sağlık Bilimleri Enstitüsü Yönetim Kurulu tarafından onaylanmıştır.

Prof. Dr. Semiha DEDE
Sağlık Bilimleri Enstitüsü Müdürü

T.C.
VAN YÜZÜNCÜ YIL UNIVERSITY
HEALTH SCIENCE INSTITUTE

**ACCEPT AND APPROVAL**

The thesis entitled **"***Investigation of Wound Healing Effect of Hyaluronic Acid/Pullulan Gel Formulations*" submitted by Saad Khalaf Matloob ALMATLOB in fulfillment of the requirements for the degree of Master of Science in the Department of Basic Pharmaceutical Sciences, Health Science Institute at Van Yüzüncü Yıl University, is hereby accepted.

Thesis Examination Date: 26/12/2023

Assoc. Prof. Dr. Mehmet BERKÖZ
Van Yüzüncü Yıl University
Chair of the Examination Committee

| | |
|---|---|
| Asst. Prof. Dr. Ömer TÜRKMEN | Assoc. Prof. Dr. Oruç YUNUSOĞLU |
| Van Yüzüncü Yıl University | Bolu Abant İzzet Baysal University |
| Member of the Examination Committee | Member of the Examination Committee |

The examination committee decision regarding the thesis was approved by the Board of Directors of Van Yüzüncü Yıl University Health Sciences Institute.

Prof. Dr. Semiha DEDE
Director of the Health Science Institute

## ETİK BEYAN

T.C.
VAN YÜZÜNCÜ YIL ÜNİVERSİTESİ
SAĞLIK BİLİMLERİ ENSTİTÜSÜ MÜDÜRLÜĞÜ'NE

Yüksek Lisans/Doktora tezi olarak hazırlayıp sunduğum "*Investigation of Wound Healing Effect of Hyaluronic Acid/Pullulan Gel Formulations*" başlıklı tezim; bilimsel ahlak ve değerlere uygun olarak tarafımdan yazılmıştır. Tezimin fikir/hipotezi tümüyle tez danışmanım ve bana aittir. Tezde yer alan deneysel çalışma/araştırma tarafımdan yapılmış olup, tüm cümleler, yorumlar bana aittir. Bu tezdeki bütün bilgiler akademik kurallara ve etik ilkelere uygun olarak hazırlanıp, bu kural ve ilkeler gereği, çalışmada bana ait olmayan tüm veri, düşünce ve sonuçlara atıf yapılmış ve kaynak gösterilmiştir.

Yukarıda belirtilen hususların doğruluğunu beyan ederim.

Öğrencinin Adı Soyadı: Saad Khalaf Matloob ALMATLOB

Tarih: 04/01/2024

İmza:

## ETHICAL DECLARATION

To The,
T.C.
VAN YÜZÜNCÜ YIL UNIVERSITY
HEALTH SCIENCE INSTITUTE DIRECTORATE,

My thesis titled "*Investigation of Wound Healing Effect of Hyaluronic Acid/Pullulan Gel Formulations*" that I prepared and presented as a Master's thesis; written by me in accordance with scientific ethics and values. The idea/hypothesis of my thesis belongs to me and my thesis advisor completely. The experimental study/research in the thesis was made by me and all sentences and comments belong to me. All the information has been prepared in accordance with academic rules and ethical principles in this thesis, and according to these rules and principles in the study; all the data, thoughts and results that doesn't belong to me have been cited and referenced.

I declare that the above-mentioned points are true.

Name and Surname (Student): Saad Khalaf Matloob ALMATLOB

Date: 04/01/2024

Signature:

## ACKNOWLEDGMENTS

At the beginning, I express my inexpressable gratitude to Allah, and deep thanks to Republic of Türkiye for giving me this opportunity to complete my master degree, and for making this dream come true.

I would like to express my sincere gratitude to my supervisor Asst. Prof. Dr. Ömer Türkmen, Department of Pharmaceutical Technology, for his scientific instruction, patience, understanding and the encouragement to do the best during the throughout this work.

I am very thankful to my co-supervisor Assoc. Prof. Dr. Mert İLHAN, Department of Pharmacognosy, Faculty of Pharmacy, Düzce University, for his great help for conducting this thesis work.

I would also like to express my deep thanks to Prof. Dr. Gökhan BORAN, Department of Food Engineering, Engineering Faculty, Van YYU for his help in conducting Texture Analysis study; to Prof. Dr. Burak KAPTANER, Department of Biology, Faculty of Science, Van YYU for his help in conducting histopathological study; to Assoc. Prof. Dr. Sakine TUNCAY TANRIVERDİ, Department of Pharmaceutical Technology, Faculty of Pharmacy, Ege University for her help in conducting rheological studies; to Asst. Prof. Dr. Leyla BEBA, Faculty of Pharmacy, Eastern Mediterranean University, North Cyprus, for her help in analysing the results; and to Asst. Prof. Dr. Abdulhamit BATTAL, Department of Pharmaceutical Biotechnology for his helpfulness and patience.

I am thankful to Prof. Dr. Yavuz YARDIM, Dean of the Faculty of Pharmacy, and every member of Faculty of Pharmacy for their support and patience.

I would like to thank the members of Supervisory Committee for their constructive advices.

I would also like to thank to members of the Van YYU Experimental Medicine Research Application Center for their help in conducting the animal studies and Van YYU Scientific Research Projects Department for financial support that gave opportunity to perform this study.

My sincere gratitude extends to my relatives, especially my mother Fatima ALSALEEM, my sister Shamsa ALMATLOB, my wife Hala ALATRAQCHI, my lovely Kids Hassan Saad ALMATLOB and Fatima Saad ALMATLOB, and to all my sisters and brothers for their endless love, their support and encouragement throughout my scientific journey from the beginning till now.

Saad Khalaf Matloob ALMATLOB

Van-2024

## TABLE OF CONTENTS

KABUL VE ONAY ..... III
ETİK BEYAN ..... V
ETHICAL DECLARATION ..... VI
ACKNOWLEDGMENTS ..... VII
TABLE OF CONTENTS ..... IX
ACRONYMS AND ABBREVIATIONS ..... XI
LIST OF FIGURES AND ILLUSTRATIONS ..... XII
LIST OF TABLES ..... XIII
1. INTRODUCTION ..... 1
2. BACKGROUND ..... 2
2.1. Phases of Wound Healing ..... 2
2.1.1. Inflammatory stage ..... 3
2.1.2. Proliferative stage ..... 5
2.1.3. Remodeling stage ..... 7
2.1.4. Epithelial-mesenchymal interaction in healing ..... 8
2.2. Factors Affecting Wound Healing Process ..... 9
2.2.1. Nutritional and environmental factors ..... 9
2.2.2. Impact of radiation and medications ..... 10
2.2.3. Genetic factors influencing wound healing ..... 11
2.3. Polysaccharides and Their Wound Healing Applications ..... 11
2.3.1. Hyaluronic acid ..... 12
2.3.2. Pullulan ..... 15
Pullulan in wound healing applications ..... 16
2.3.3. Wound healing applications based on hyaluronic acid and pullulan ..... 17
2.4. Main Purpose of the Study ..... 18
3. MATERIALS AND METHODS ..... 20
3.1. Materials ..... 20
3.2. Methods ..... 21
3.2.1. Formulation approach for the development of gels ..... 21
3.2.2. Gel preparation ..... 21
3.2.3. Texture profile analysis ..... 22
3.2.4. Data analysis and experimental design optimization studies ..... 23

3.2.5. Further examination of optimized gel formulations ..... 23
3.2.6. *In vivo* experiments ..... 24
3.2.7. Statistical analysis ..... 26
4. RESULTS ..... 27
4.1. Assessment of the Box-Behnken Experimental Design ..... 27
4.2. Texture Analysis Data Obtained with Selected Formulations ..... 30
4.3. Validation of the model employed with selected formulations ..... 32
4.4. Further examination of the optimized gel formulations ..... 33
4.4.1. pH measurement of the optimized gel formulations ..... 33
4.4.2. Differential scanning calorimetry analysis ..... 33
4.4.3. Rheological Evaluation of the Optimized Gel Formulations ..... 35
4.4.4. *In Vivo* experiments ..... 37
5. DISCUSSION AND CONCLUSION ..... 42
5.1. Texture Profile Analysis Study and Assessment of the Box-Behnken Experimental Design ..... 42
5.2. Further Examination of the Optimized Gel Formulations ..... 45
5.2.1. pH measurement of the optimized gel formulations ..... 45
5.2.2. Differential scanning calorimetry analysis ..... 45
5.2.3. Rheological evaluation of the optimized gel formulations ..... 46
5.3. *In Vivo* Experiments ..... 48
SUMMARY ..... 51
GENİŞLETİLMİŞ TÜRKÇE ÖZET ..... 52
(EXTENDED SUMMARY IN TURKISH) ..... 52
ÖZET ..... 52
1. GİRİŞ ..... 53
2. GENEL BİLGİLER ..... 53
3. GEREÇ ve YÖNTEM ..... 57
4. BULGULAR ..... 60
5. TARTIŞMA VE SONUÇ ..... 62
REFERENCES ..... 66
RESUME ..... 73
APPENDIX ..... 74

## ACRONYMS AND ABBREVIATIONS

| | | |
|---|---|---|
| **ANOVA** | **:** | Analysis of Variance |
| **BBED** | **:** | Box-Behnken Experimental Design |
| **DOE** | **:** | Design of experiments |
| **DSC** | **:** | Differential Scanning Calorimetry |
| **ECM** | **:** | Extracellular matrix |
| **EMT** | **:** | Epithelial-mesenchymal transition |
| **FDA** | **:** | U.S. Food and Drug Administration |
| **FGF** | **:** | Fibroblast growth factor |
| **GAG** | **:** | Glycosaminoglycan |
| **GLY** | **:** | Glycerol |
| **GRAS** | **:** | Generally Recognized as Safe |
| **HA** | **:** | Hyaluronic Acid |
| **H&E** | **:** | Hematoxylin and Eosin |
| **kcal** | **:** | Kilocalorie |
| **MW** | **:** | Molecular weight |
| **NSAIDs** | **:** | Non-steroidal anti-inflammatory drugs |
| **PDGF** | **:** | Platelet-derived growth factor |
| **PGE2** | **:** | Prostaglandin E2 |
| **PUL** | **:** | Pullulan |
| **TA** | **:** | Texture Profile Analysis |
| **TGF β** | **:** | Transforming growth factor-beta |
| **UDP** | **:** | Uridine diphosphate |
| **UDP-N** | **:** | Uridine diphosphate N-acetylglucosamine |
| **VEGF** | **:** | Vascular endothlial growth factor |
| **3DR** | **:** | Three dimensional response |

## LIST OF FIGURES AND ILLUSTRATIONS

**Figure 1.** The sequential steps involved in tissue repair ..... 3

**Figure 2.** Chemical structure of hyaluronic acid. ..... 14

**Figure 3.** The chemical structure of pullulan. ..... 16

**Figure 4.** The experimental setup used for Texture Profile Analysis study ..... 23

**Figure 5.** 3D surface plot representation of the relationship between independent variables and firmness response. ..... 28

**Figure 6.** 3D surface plot representation of the relationship between independent variables and adhesive force response. ..... 28

**Figure 7.** 3D surface plot representation of the relationship between independent variables and spreadability response ..... 29

**Figure 8.** 3D surface plot representation of the relationship between independent variables and adhesiveness response. ..... 29

**Figure 9.** TA plot obtained for F1 ..... 30

**Figure 10.** TA plot obtained for F2 ..... 30

**Figure 11.** TA plot obtained for F3. ..... 31

**Figure 12.** TA plot obtained for F4 ..... 31

**Figure 13.** TA plot obtained for F5 ..... 32

**Figure 14.** TA plot obtained for F6 ..... 32

**Figure 15.** Differential scanning calorimetric thermograms of the HA and PUL, physical mixture of HA and PUL and gel formulations ..... 34

**Figure 16.** Viscosity changes over shear rate of a. F1; b. F2; c. F3; d. F4; e. F5; and f. F6 formulations at 25ºC. ..... 35

**Figure 17.** Flow curves of a. F1; b. F2; c. F3; d. F4; e. F5; and f. F6 formulations at 25ºC ..... 35

**Figure 18.** Viscosity changes over shear rate of formulations a. F1; b. F2; c. F3; d. F4; e. F5; and f. F6 formulations at 32ºC. ..... 36

**Figure 19.** Flow curves of a. F1; b. F2; c. F3; d. F4; e. F5; and f. F6 formulations at 32ºC ..... 36

**Figure 20.** The images of circular excision wounds at different days. ..... 38

**Figure 21.** The representative photomicrographs of the skin from wound areas in the experimental groups ..... 41

## LIST OF TABLES

**Table 1.** The role of hyaluronic acid in wound healing process ..... 15
**Table 2.** The materials used in the study ..... 20
**Table 3.** The instruments used in the study ..... 20
**Table 4.** Variables of the BBED Matrix ..... 21
**Table 5.** Responses of the BBED Matrix ..... 27
**Table 6.** Regression equations of fitted models of the BBED Matrix ..... 27
**Table 7.** Validation of the model employed with selected formulations ..... 33
**Table 8.** The percentage contraction effects of the applied agents on the area of circular excision wound model in mice ..... 37
**Table 9.** Scoring of the histopathological findings in the skin sections of the different experimental groups. ..... 38

# 1. INTRODUCTION

Skin is the largest organ of the human body, with a main key function to protect water-rich internal organs from the external environment with low humidity. For a healthy survival, maintaining skin integrity and possessing a strong wound healing capability are key prerequisites. When the integrity of the skin and any tissue is damaged, this is described as wound. Besides, the significance of wound care can also be highlighted because of its major challenge with a significant burden on health care systems. The highest wound-related expenses are attributed firstly to the surgical wounds and secondly to the diabetic foot ulcers (Almadani et al., 2021).

The wound healing process is the series of synchronized manifestations to restore the integrity of skin. This section focused on the overall process occurs in the acute cutaneous wound healing. This is described firstly under the title of ‘’Phases of Wound Healing’’ in detail. Thereafter, the factors having impact on the wound healing process followed by polysaccharides in wound healing were discussed.

# 2. BACKGROUND

## 2.1. Phases of Wound Healing

As an important physiological process, cutaneous wound healing involves the cooperation of numerous cell types and their byproducts (Shaw and Martin, 2009; Gonzalez et al., 2016). Early on in the inflammatory stage, efforts are made to repair the lesion caused by a local injury. This includes employing stem cells or already-existing tissue cells to replace the specialized structures made by collagen deposition and regeneration, which is the process of cell proliferation and posterior differentiation. (Eming et al., 2007). These stages do not exclude one another mutually, meaning that following a skin lesion, depending on the cell type affected by the injury, regeneration and repair may take place in the same tissue (Gonzalez et al., 2016).

Following the beginning of the injury, processes of tissue regeneration and repair take place, because of the trauma or as a consequence of a particular clinical state. All the stimuli that disrupt the physical continuity of functioning tissues results in a single lesion. Internal or external factors that are physical, chemical, electrical, or thermal can be causative factors for lesions, which also may be harmful to particular organelles or to the cells in their entirety (Shaw and Martin, 2009). Tissue repair is characterized by a simple linear process, at which cell proliferation is induced by growth factors, leading to the integration of dynamic changes involving soluble mediators, blood cells, extracellular matrix production, and proliferation of parenchymal cells. The skin healing process is an illustrative example of the principles that occurs in the repairment process of the majority of tissues (Kumar et al., 2020). The cellular and physiological processes involved in wound repair can be divided into three stages: the inflammatory response, the formation of extracellular matrix components and cell proliferation, and a final stage known as remodeling (Nayak et al., 2009). These phases overlap over time rather than being mutually exclusive as depicted by Gonzalez *et al*. (Figure 1) (Gonzalez et al., 2016).

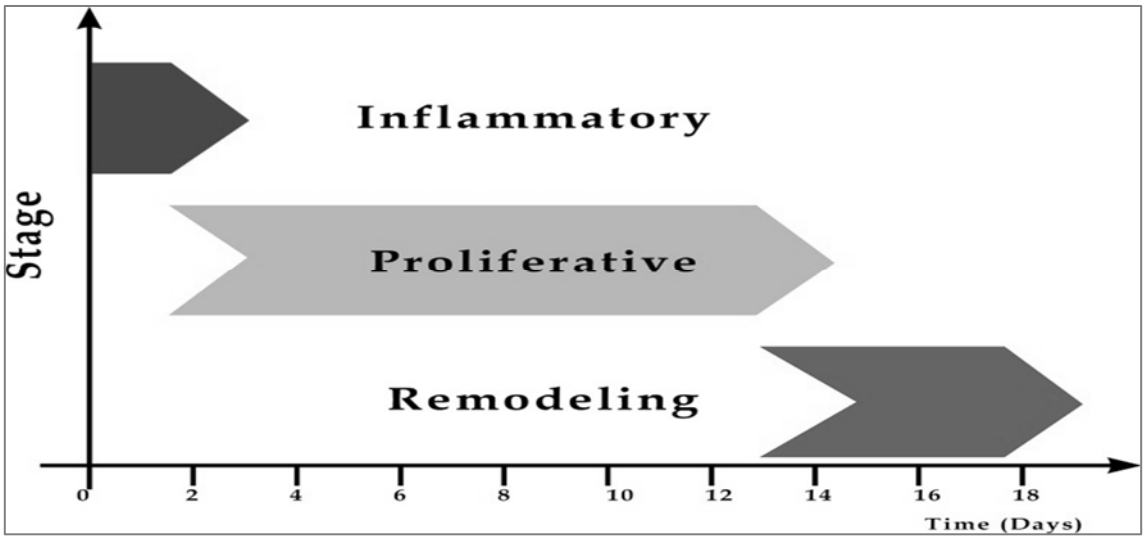


**Figure 1.** The sequential steps involved in tissue repair

### 2.1.1. Inflammatory stage

In the inflammatory stage, the ruptured blood vessels and the leaking blood coagulates preserve the integrity during a vascular inflammatory reaction. A fibrin network is formed when thrombocytes and platelets aggregate during coagulation, and this process is dependent on certain stimuli that cause these cells to become activated and aggregated (Medrado et al., 2003). Apart from restoring homeostasis and creating a barrier against microbial invasion, the fibrin network also facilitates cell migration by arranging the temporary matrix required for the process. This ultimately reinstates the role of the skin as a protective barrier and preserves the integrity (Shaw and Martin, 2009). Additionally, this allows the stimulation of fibroblast proliferation and cell migration to the microenvironment of lesion (Gonzalez et al., 2016).

The influx of leukocytes into the area of the wound indicates the cell response, which occurs extremely quickly and is consistent with the classic indicators of inflammation including erythema and edema where the lesion is located. Cell response usually takes up to two days to completely develop, but it is established during the first 24 hours. Rapid activation of the immune cells within the tissue can also occur, as chemokines and cytokines are secreted by mastocytes, gamma-delta cells, and Langerhans cells. The lesion releases inflammation, a protective and limited tissue response that results in tissue damage. In addition to aiding in the release of lysosomal enzymes and reactive oxygen species and in the removal of different cell debris,

inflammatory cells are crucial for the wound healing (Medrado et al., 2003; Gonzalez et al., 2016).

Neutrophils are actively recruited as a part of the inflammatory response in response to the activation of the complement system, platelet degranulation, and products of bacterial breakdown (Gurtner et al., 2008). Numerous inflammatory cytokines released by endothelial cells, activated platelets, and degradation products of the pathogenic agents (Nunes et al., 2011). As a result, the neutrophils are the main cells that are recruited and activated to aid in tissue cleanup and the destruction of invasive pathogens (Kumar et al., 2020).

Many neutrophils migrate through blood capillary wall endothelial cells a few hours after the lesion occurs. These cells are activated by pro-inflammatory cytokines such as interferon gamma (IFN-γ), tumor necrosis factor alpha (TNF-α), and IL-1 β near the lesion site. These cytokines stimulate the expression of numerous adhesion molecule types. Selectins and integrins are two of these adhesion molecules that interact with those existing on the membrane surface of endothelial cells to determine the diapedesis of neutrophils (Eming et al., 2007; Gonzalez et al., 2016). Numerous other mechanism of tissue repair, including the resolution of fibrin and extracellular matrix coagulation, the stimulation of angiogenesis, and reepithelialization, are also influenced by the referent cells (Shaw and Martin, 2009).

After 48 hours, monocytes from nearby blood arteries that have also infiltrated the lesion area begin to migrate more intensely. As a result of the formation of new genic expression patterns, these monocytes eventually differentiate into macrophages. These cells can function as antigen-presenting entities and assist neutrophils in phagocytosis when they are stimulated by chemokine signaling (Eming et al., 2007; Gonzalez et al., 2016).

Macrophages carry out the phagocytosis of muscle detritus in addition to producing and releasing pro-angiogenic, inflammatory, fibrogenic, and cytokines as well as free radicals (Tidball, 2005). Furthermore, additional inflammatory cells are drawn to the wound site via macrophages by secreting chemotactic proteins. Additionally, prostaglandins are formed, which have the ability to significantly reduce permeability of

blood vessel by acting as powerful vasodilators. These elements work together to activate endothelial cells (Li et al., 2007). It has been reported that these cells also secrete PDGF, TGF beta, FGF, and VEGF, which are notable for being the primary cytokines that can promote the development of granulation tissue (Gonzalez et al., 2016).

### 2.1.2. Proliferative stage

This stage aims to create a viable epithelial barrier to activate keratinocytes by contracting and fibroplasia, hence decreasing the lesioned tissue area. The lesion's actual closure, which involves fibroplasia, reepithelialization, and angiogenesis, is the result of this stage. These processes start in the lesion microenvironment during the first 48 hours, and can continue until the 14th day of lesion (Li et al., 2007).

Vascular remodeling induces modifications in blood flow. Angiogenesis is a well-coordinated process that includes the recruitment of perivascular cells, migration and interaction in tubular structures, rupture and reorganization of the basal membrane, and the proliferation of endothelial cells. Angiogenesis has long been considered necessary for a variety of physiological and pathological processes, including metastasis, tumor growth, and embryogenesis (Rosen, 2002).

The germination and cell division are the two processes that produce collateral veins during the subsequent development of the blood vessels (Gonzalez et al., 2016). The resulted vascular plexus is altered to distinguish between large and small blood vessels, and then smooth muscle and auxiliary cells fill in the endothelium. Transportation of fluid, oxygen, nutrients, and immune-competent cells to the stroma is made feasible by the newly developed microvasculature (Carmeliet, 2003).

In addition to lymphocytes and endothelial cells actively participating in this biological process, pericytes are a cell group that originates from smooth muscle cells of the mesenchymal strain. Though they look as separate entities, these cells share the blood artery and endothelial cells' basal membrane. The pericytes are light-colored connective tissue cells that have long, thin cytoplasmic processes that are found directly outside the endothelium of capillaries and tiny venules into which the blood capillaries empty themselves (Ribatti et al., 2011; Alon and Nourshargh, 2013). The pericyte makes focal

contact with the endothelium by specialized junctures, which are lengthy cytoplasmic extensions that stretch and surround the endothelial tube. Furthermore, this type of cell affects blood vessel integrity by depositing matrix and/or releasing and activating signals that encourage endothelial cell compliance or differentiation (Gonzalez et al., 2016).

Approximately four days following the occurence of lesion, formation of granulation starts, name of which comes from the newly created granular appearance of tissue that gives the nascent stroma this feature. Understanding the tissue repair process requires mentioning certain immune system charateristics, like the involvement of B lymphocytes and, more especially, the multifunctionality of T lymphocytes. When a tissue lesion occurs, a range of cytokines and growth factors that affect migration, proliferation, and local cell differentiation as well as the cell activity of the inflammatory response of the cells on the lesion boundaries (eg. keratinocytes) take place, all of which affect the repair process (Mason et al., 2002; Gonzalez et al., 2016).

Angiogenesis is the result of endothelial cell migration and mitogenic activation in the extracellular matrix of the wound bed. Such neovascularization occurs concurrently with the previously described fibroblastic stage. Proper irrigation of the margins of wound is crucial for wound healing because it provides the stroma with an appropriate supply of nutrients, oxygen, and immune-competent cells (Ruiter et al., 1993; Tonnesen et al., 2000).

Re-epithelialization is the process by which the epithelial covering cells multiply and move away from the wound's edges in an effort to close it, taking part concurrently with all of the previously described activities. This process is triggered by certain cytokines and combining the proliferative stage with the migration of cells close to the lesion allows keratinocytes to re-epithelialize a wound. Keratinocytes move in the direction of the intact skin toward the extremities of the lesion. Hair follicle epidermal cells quickly act to eliminate coagulation and injured stroma. The epidermal germ cells of the hair follicle give rise to the hair bulb to act as a reservoir for keratinocytes during the healing process. Actin filaments begin to develop in the extremities of the cytoplasms, the tonofilaments retract, the extracellular matrix-cell and cell-cell connections vanish, and the pseudopod projections of keratinocytes start to grow and stretch about 10 hours after the lesion occurs. When the migration stops, the keratinocytes reconnect to the

substrate and reconstruct, possibly due to contact-induced inhibition (Li et al., 2007; Landén et al., 2016).

### 2.1.3. Remodeling stage

Remodeling, which can take up to a year to complete, is the third stage of healing and starts two to three weeks after the lesion first appears. Achieving the highest tensile strength through extracellular matrix reconfiguration, breakdown, and resynthesis is the main goal of the remodeling stage. At this last stage of the lesion's healing process, the granulation tissue undergoes a slow remodeling process in an effort to restore the normal tissue structure. This results in scar tissue that is less cellular and vascular, showing a progressive increase in the concentration of collagen fibers (Gonzalez et al., 2016; Landén et al., 2016; Kumar et al., 2020).

The initial inflammation resolves and the components mature, resulting in significant alterations to the extracellular matrix. Epidermal migration stops at the lesion surface when a monolayer of keratinocytes forms, and a new stratified epidermis with a subjacent basal lamina forms from the borders of the wound into the interior (Martin, 1997; Gonzalez et al., 2016; Landén et al., 2016). At this stage, the matrix is depositing and changing in composition. As a result Type III collagen is broken down, which give rise to synthesis of the type I collagen as wound closes (Li et al., 2007). Hyaluronic and fibronectic acid levels decrease during remodeling. These substances are broken down by cells and plasmatic metalloproteinase, while the previously noted increase in type I collagen expression is simultaneously processed (Gonzalez et al., 2016).

Because most blood vessels, fibroblasts, and inflammatory cells leave the wound area due to immigration processes, apoptosis, or other unknown cell death mechanisms, fewer cells proliferate in the scar during the maturation and remodeling phases. The fibroblasts in the granulation tissue eventually undergo a phenotypic change and briefly start to make smooth muscle actin; these cells are then known as myofibroblasts. (Medrado et al., 2003; Calin et al., 2010).

It is crucial to stress that both endogenous and external factors have the ability to modulate such events and affect the healing process in all of the processes mentioned

above. More precisely, the early closure of the wound might be impeded by systemic illnesses including diabetes, immunosuppression, venous stasis as well as those due from exogenous agents like smoking and corticotherapy use as discussed in the following sections (Gonzalez et al., 2016; Landén et al., 2016).

### 2.1.4. Epithelial-mesenchymal interaction in healing

The epithelial cells migrate to the organs to differentiate into their mesenchymal components, such as fibroblasts, blood vessel smooth muscle cells, and, more likely, pericytes, after undergoing an epithelial-mesenchymal transition (EMT). Mesenchymal and epithelial cells are found in the skin, intestines, liver, lungs, and glandular organs. The basoapical polarity is visible in the layers that are formed by the tightly adhering epithelial cells. Because there are no longer any intercellular connections, mesenchymal cells are non-polarized and able to migrate individually (Chong et al., 2009; Gonzalez et al., 2016).

Molecular changes can occur in a polarized epithelial cell during the EMT process, resulting in the acquisition of a mesenchymal phenotype. This phenotype includes the ability to migrate through the extracellular matrix, resistance to apoptosis, and increased production of matrix constituents (Choi and Diehl, 2009). There are three recognized forms of EMT. The dermal fibroblasts of the connective tissue, which offer identifying signals for placement, skin types, and other skin appendages that will differentiate themselves into the overarching epidermis, demonstrate that type I arises when the tissues are created during embryogenesis (Martin, 1997). In adult tissues, the epithelial-mesenchymal transition also happens in response to remodeling and type II fibrosis (Choi and Diehl, 2009). Using the EMT program, which typically produces adult fibroblasts, carcinoma cells that undergo phenotypic conversion and acquire motility are part of the metastatic process (type III) (Zeisberg and Neilson, 2009; Gonzalez et al., 2016).

Fibrosis, regeneration, and type II EMT are all linked to the tissue repair. This process, which is associated with tissue healing, produces fibroblasts and other cells that are involved in the goal of rebuilding tissues that have been damaged by inflammation and trauma. This kind of inflammatory EMT stops as soon as the inflammation is reduced.

There are also theories that microfibroblasts can create the transmembrane protein known as the Hedgehog ligand. This regulates the survival and migratory activity of different cell types that respond to the hedgehog ligand and also governs tissue remodeling and creation (Sicklick et al., 2006; Gonzalez et al., 2016).

### 2.2. Factors Affecting Wound Healing Process

#### 2.2.1. Nutritional and environmental factors

The wound healing process requires high energy and a healthy nutritional condition. Both macronutrients and micronutrients are required for this process in order to support the repair of skin integrity. A healthy wound healing process depends on macronutrients like carbonhydrates, lipids, proteins, and fluids as well as micronutrients like vitamins, minerals, and amino acids. The estimated total energy needed to synthesise proteins is 0.9 kcal/g, and 10 mg of collagen would be needed to cover a portion of granulation tissue that is 1 mm thick (Almadani et al., 2021).

Thus, whereas tiny wounds might not always present a nutritional difficulty, as wounds get larger especially in the case of large thermal burns, the nutritional shortfall starts to get wider. This is a crucial factor to take into account for patients who may have fasted for an extended amount of time after surgery, and it might be advantageous to have an early conversation with patients about starting a new diet (Ahmed, 2005). As uncontrolled hyperglycemia has been demonstrated to decrease fibroblast and endothelial cell activity in poorly managed diabetic individuals, tight glycemic regulation is essential for optimal wound healing (Williams and Barbul, 2003; Arnold and Barbul, 2006).

Since cigarattes contain over 400 compounds, smoking may pose harmful affects on the wound healing process. In particular, nicotine substantially stimulates vasoconstriction, which interferes with microcirculation and impairs the healing of wounds. Moreover, smoking inhibits neutrophil activity and cellular migration during the inflammatory stage of wound healing. In general, smokers experience more difficulties in healing of wounds than nonsmokers (Silverstein, 1992; Almadani et al., 2021). Smoking affects the tissue microenvironment transiently, but it also has a long-term impact on the functioning of reparative and inflammatory cells, which causes problems

and a delayed healing. Within four weeks of smoking cessattion, the inflammatory cellular activities and tissue microenvironment are restored, but the proliferative response is not improved. Also, nicotine appears to reduce inflammation and promote proliferation, but it has no effect on the tissue microenvironment (Sørensen, 2012).

In contrast to the well-established effects of smoking, the negative consequences of excessive alcohol consumption on wound healing are just now being acknowledged and investigated. Patients who have previously alcohol abuse were shown to be more likely to have infections of surgical wound. Furthermore, some research suggests that acute alcohol intoxication rather than merely chronic abuse may be harmful to the healing of wounds (Guo and DiPietro, 2010; Jung et al., 2011; Almadani et al., 2021). Among alcohol abusers, the protein level of the wound healing process is reversible after withdrawal (Tønnesen et al., 2012).

### 2.2.2. Impact of radiation and medications

Ionizing radiation can disrupt single or double strands of DNA or cause the double helix to become crosslinked. This is caused by excited subatomic particles. Additionally, free radicals produced by radiation harm cell membranes and proteins. This has an impact on fibroblasts and other wound-healing cells, impairing their migration, contraction, and proliferation. The aforementioned anomalies result in insufficient wound healing, delayed epithelialization, reduced tensile strength, elevated infection, and dehiscence rates (Tibbs, 1997; Vignard et al., 2013; Almadani et al., 2021).

It is thought that radiation and chemotherapy mostly affect skin cells that divide quickly, such as keratinocytes, as well as fibroblasts, melanocytes, endothelial cells, and immune cells. Chemotherapeutic drugs negatively impact and postpone the inflammatory stage of wound healing, which results in decreased collagen production and fibrin deposition as well as delayed wound contraction (Deptuła et al., 2019; Almadani et al., 2021). However, it has been reported that in patients receiving a neoadjuvant therapy, there was no increase in wound complications after breast surgery (Decker et al., 2012).

Several of the most often prescribed drugs may hinder the healing of wounds. It has been demonstrated that nonsteroidal anti-inflammatory medications (NSAIDs) inhibit

the healing of wounds, by inhibiting COX-1 and COX-2 as well as reducing PGE2 synthesis, as shown with preclinical evidence. As a result, they may prevent tissue repair by delaying the inflammation. Crucially, NSAIDs may slow the process of healing by having an antiproliferative effect on angiogenesis. It should be noted that patients with diabetes or chronic wounds may be more severely susceptible to the NSAID's effect on fibroblast inhibition. Short-term use of the NSAID may be helpful for controlling acute pain with little consequence on the wound healing (Su et al., 2010; Almadani et al., 2021). This approach is also applied to steroids, where administration of systemic corticosteroids at large doses over an extended period of time is expected to have little clinical impact on wound healing (Wang et al., 2013). Steroids and vitamin A have opposing effects on wound healing, and vitamin A can counteract the effects of steroids (Wicke et al., 2000).

### 2.2.3. Genetic factors influencing wound healing

Patients with a number of inherited connective tissue abnormalities are more likely to experience issues with wound healing. Cutis laxa is characterized by increased dermal vascularization, reduced collagen bundle size, underdeveloped elastic fibers, and in some severe cases, may result in suboptimal wound healing. Nevertheless, for the majority of Cutis laxa patients many of whom will be able to heal normally or nearly normally, Cutis laxa does not preclude elective surgery (Morava et al., 2009; Almadani et al., 2021). Another illnesses known as Ehlers-Danlos syndrome are distinguished by anomalies in the structure of collagen, characterized by tissue fragility, skin hyperextensibility, and joint hypermobility are its defining characteristics (Callewaert et al., 2008). Furthermore, hyperhomocysteinemia may be a separate risk factor for less than ideal wound healing and may cause thrombosis, thus preventing the healing tissue to uptake necessary nutrients, particularly in wounds involving the lower extremities (Schwartzfarb and Romanelli, 2008). A list of conditions resulting in the poor wound healing process is provided by National Institutes of Health (NIH) (NIH, 2023).

## 2.3. Polysaccharides and Their Wound Healing Applications

Polysaccharides are stereoregular polymers consist of monosaccharides, which are extracted from plants, algae, animals, fungi, or obtained via fermentation. They are used for many purposes, such as dietary fibers, stabilizing agents, thickeners, emulsifiers,

coating agents, and packaging films. Plant cellulose and chitosan are affordable and readily available, making them unique raw ingredients in pharmaceuticals and cosmetics (Ribeiro et al., 2019; Tudu and Samanta, 2022).

Some of the features of polysaccharides that enable their employment as therapeutic agents are their chirality, chelation, adsorption capacity, strong chemical reactivity, polyfunctionality, biocompatibility, biodegradability, and non-toxicity. Four characteristics of polysaccharides contribute to their excellent adsorption behavior: (1) high hydrophilicity; (2) a large number of functional groups (acetamido, primary amino, and/or hydroxyl groups); (3) high chemical reactivity of these functional groups; and (4) flexible polymer chain structure (Ribeiro et al., 2019).

An extensive research has focused on the application of polysaccharides as hydrogel, gel, and membrane forming agents for a variety of purposes. Polysaccharide-based membranes, for instance, are used in the pharmaceutical industry as wound dressings thanks to their advantageous features. Polysaccharide-based formulations that employed in the treatment of wounds in animal models and clinical trials generally based on cellulose and derivatives, alginates, collagen, chitosan and derivatives, dextran, hyaluronic acid, pullulan and the others. All of which are used solely or in combination for the development of gels, hydrogels, dressings, films, scaffollds, topical sprays (Ribeiro et al., 2019; Cui et al., 2022; Elangwe et al., 2023).

Among these polysaccharides, hyaluronic acid and pullulan were selected for their unique properties in topical and wound healing applications as discussed in the following sections in detail.

### 2.3.1. Hyaluronic acid

The glycosaminoglycan (GAG) from the vitreous humor of the bovine eye was originally isolated in 1934, which was then named as "hyaluronic acid" (derived from hyaloid [vitreous] and uronic acid). In 1986, the word "hyaluronan" was introduced in order to comply with the nomenclature. Later, different tissues (nerve, connective, and epithelial) and organs (joints, skin, rooster comb, human umbilical cord, etc.) that contain hyaluronan were discovered. Additionally, hyaluronic acid (HA) is obtained by microbial

fermentation process (*Streptococcus zooepidemicus, Escherichia coli, Bacillus subtilis*, and others) (Sugahara et al., 1979; Necas et al., 2008; Gupta et al., 2019).The concentration of UDP-N-acetylglucosamine is claimed to govern the molecular weight (MW) of HA (Chen et al., 2009). Its chemical structure is same in bacteria and vertebrates (Gupta et al., 2019). The synthesis HA by the majority of body cells at some time during their cell cycles suggests that HA is involved in a number of essential biological activities (Chen, 2002; Liang et al., 2016; Fallacara et al., 2017; Fallacara et al., 2018). HA is a significant part of the extracellular matrix (ECM) and is typically found in synovial fluid, articular cartilage, and the bone marrow of mammals (Gupta et al., 2019)

HA is a non-protein molecule with repeating β-1,4-D-glucuronic acid and β-1,3-N-acetylglucosamine units, which are uronic acid and aminosugar. They are connected by alternating beta-1,4 and beta-1,3 glycosidic linkages (Figure 2). Due to the spatial relationship between the two sugars, all of the small hydrogen atoms occupy less sterically favorable axial positions when all of the bulky groups of glucose—the hydroxyls, the carboxylate moiety, and the anomeric carbon on the adjacent sugar—can be found in sterically favorable equatorial positions in the beta configuration. Consequently, the structure of the disaccharide is very energetically stable (Necas et al., 2008). Also, using the activated nucleotide sugars (UDP-glucuronic acid and UDP-N-acetylglucosamine as substrates), hyaluronan synthase enzymes synthesis large, linear polymers of the repeating disaccharide structure of hyaluronan by alternating addition of glucuronic acid and N-acetylglucosamine to the growing chain. A whole hyaluronan molecule can include up to 10,000 repeated disaccharides and a molecular mass of around 4 million daltons (each repeated disaccharide is approximately 400 daltons). A disaccharide has an average length of about 1 nm, and if a hyaluronan molecule with 10,000 repetitions were stretched end to end, it would have a length of 10 μm, which is roughly equivalent to the diameter of a human erythrocyte (Necas et al., 2008).

It possess unique physico-chemical properties, such as excellent viscoelasticity, a high capacity to retain moisture, strong biocompatibility, and hygroscopic nature. High viscosity can be produced by HA chains at concentrations as low as 0.1%. HA functions as a lubricant, shock absorber, joint structure stabilizer, and regulator of water balance and flow resistance thanks to these features (Liang et al., 2016; Gupta et al., 2019).

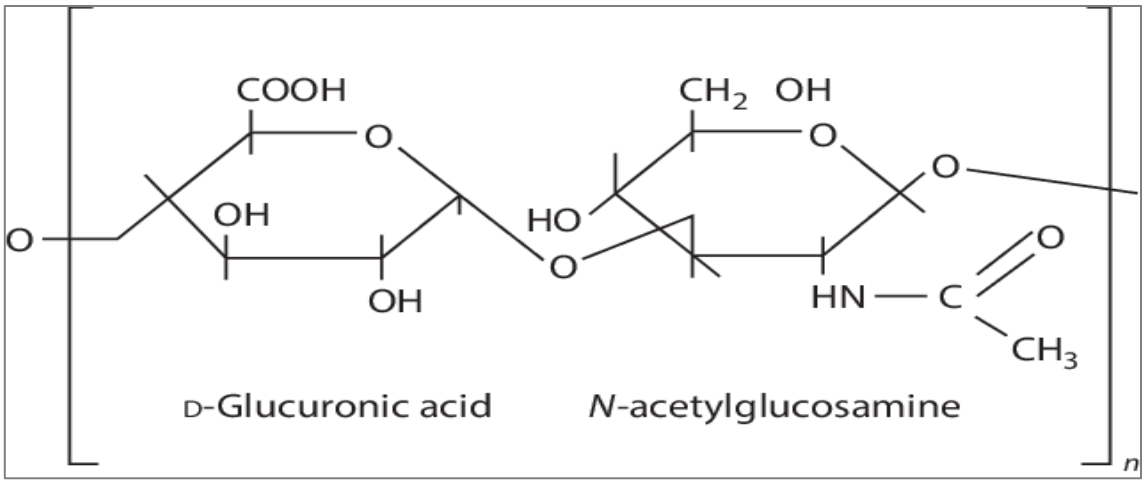


**Figure 2.** Chemical structure of hyaluronic acid.

**Pharmacotherapeutics of hyaluronic acid**

In healthy biological conditions, HA has many functions including filling up empty spaces, keeping bodies hydrated, lubricating joints, and creating a matrix that allows cells to migrate. During tissue injurence, HA is actively generated and controls both tissue healing and disease processes, including the activation of inflammatory cells to mount an innate response to damage as well as the activation of fibroblasts and epithelial cells (Liang et al., 2016). HA is utilized and underinvestigation in a range of conditions as follows: osteoarthritis; ophtalmic conditions, chemoprevention and cancer therapy, wound healing, cardiovascular applications, and so on (Chen, 2002; Liang et al., 2016; Fallacara et al., 2017; Fallacara et al., 2018).

**Hyaluronic acid in wound healing**

GAG-containing hyaluronan is an extracellular polysaccharide implicated in wound healing. The structure and physiology of HA are key requirements to understand its role in wound healing. The repeating units of D-glucuronic acid and N-acetylglucosamine make HA as a negatively charged disaccharide polymer *in vivo* (Frenkel, 2014). There are different lengths of HA polymers, and every molecular size has a distinct function on every stage of wound healing. In brief, large HA molecules have structural regulatory roles with space filling, while small HA fragments are connected to inflammation and immunostimulation (Stern et al., 2006). The role of HA in wound healing process is summarized in Table 1 (Frenkel, 2014).

**Table 1.** The role of hyaluronic acid in wound healing process

| Phase | Effect in Process |
|---|---|
| Inflammatory | Binds with fibrinogen to start the blood clotting process.<br>Permits movement of inflammatory cells.<br>Causes oedema to facilitate cell penetration.<br>Inhibits the migration of neutrophils to reduce the inflammatory response. |
| Proliferative | Attracts fibroblasts to the area of injury<br>Fills in the gaps of recently formed ECM, thereby provides structural organization and cushioning.<br>MMPs are stimulated for angiogenesis.<br>Promotes the migration and proliferation of keratinocytes. |
| Remodelling | Plays role in normal and pathological scarring. |

**Hyaluronic acid in wound healing applications**

In addition to its function in the wound healing process, characteristics of HA have been effectively applied in a variety of wound dressings and other products recently (Graça et al., 2020). Current commercial examples of HA-containing products include Bionect®, Connettivina®, Hyalofill®, Hyalomatrix®, Hyalosafe®, Hylase Wound Gel®, HylaSponge®, Laserskin®, Ialuset®, Hyiodine®, all of which have been investigated and proven to be clinically efficacious in a range of wounds (Frenkel, 2014; Graça et al., 2020). Also some experimental examples includes hydrogels, sponges, films and electrospun membranes (Graça et al., 2020).

### 2.3.2. Pullulan

Pullulan (PUL) is a α-D-glucan produced by a polymorphic fungus, *Aureobasidium pullulans*. The principles underlying this organism's biosynthesis of PUL have been thoroughly examined (Cheng et al., 2011; Li et al., 2015; Wei et al., 2021). It is a naturally occurring biopolymer, which is characterized by colorless, odorless, non-toxic, non-carcinogenic, extremely biocompatible, and biodegradable properties. In addition to having distinctive physico-chemical properties, it is environmentally friendly. A lengthy chain of glucopyranose rings connected by two different kinds of linkages-α-(1 → 6) and α-(1 → 4-makes up the pullulan structure. The distinct features of PUL are attributed to the existence of both α-(1 → 6) and α-(1 → 4) links in its structure. The hydrolytic enzymes known as "pullulanases" have a strong effect on its structure. Maltose, isomaltose, maltotriose, maltotetraose, panose, and isopanose, its many structural units, are debranched by pullulanases during partial hydrolysis. Maltotriose is

typically the repeating unit in PUL structures. Three α-(1 → 4) linked glucopyranose rings connected by α-(1 → 6) glycosidic linkages make up each maltotriose unit. Regular modification of α-(1 → 4) and α-(1 → 6) bonds accounts for its structural adaptability and improves PUL disintegration. The chemical structure of PUL is shown in Figure 3. PUL has special capabilities due to this particular glycosidic bond, including the ability to form fibers, compression moldings, and long-lasting films that are impermeable to oxygen. The physico-chemical properties of PUL can be improved with modifications in its structure through a variety of chemical processes (Singh et al., 2023).

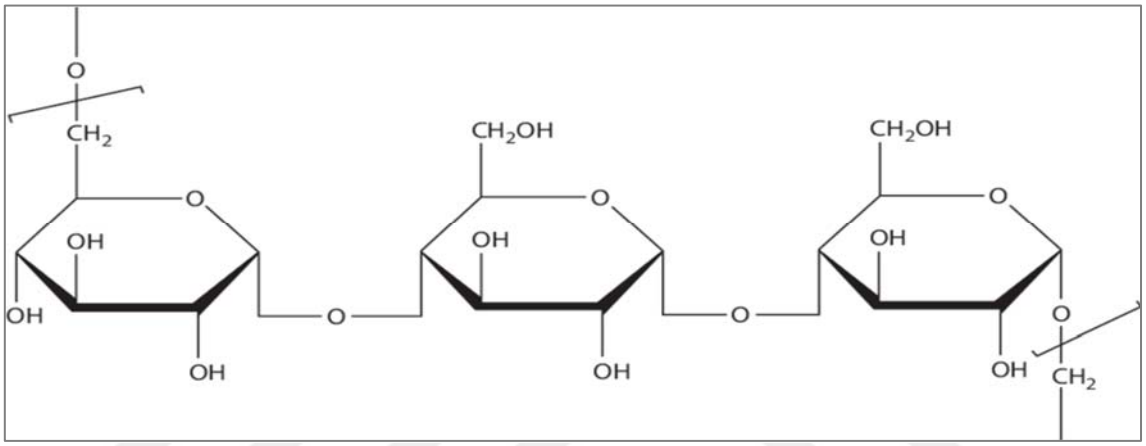


**Figure 3.** The chemical structure of pullulan.

The US FDA has listed this biopolymer in Generally Recognized as Safe (GRAS) category. It is regarded as an essential polymer for industrial usage because of its unique qualities and GRAS certification. It has promising pharmaceutical and biomedical, food, cosmeceutical and health care applications (de Souza et al., 2023; Singh et al., 2023). Thanks to these properties, PUL has found a wide range of applications in both pharmaceuticals and cosmeceuticals. The detailed applications of PUL in various delivery routes as well as in cosmeceuticals were thoroughly reviewed (de Souza et al., 2023; Singh et al., 2023).

**Pullulan in wound healing applications**

Naturally occurring polymers are commonly employed in the design and production of wound dressings thanks to their characteristics that are similar to those of the ECM and are not immunogenic like synthetic polymers (Mano et al., 2007; Frenkel, 2014; Mogoşanu and Grumezescu, 2014; Graça et al., 2020). PUL-based hydrogels with

various polysaccharides, including chitosan, chitin, gelatin, and collagen in wound healing and skin tissue engineering applications have recently attracted significant attention. These are utilized in the development of films, sponges, and hydrogels for use as skin tissue scaffolds, wound dressings, and drug delivery systems. PUL and other polymers, including chitosan, have advantageous features, which makes the hydrogel composites made of these polysaccharides can significantly improve the wound healing (Elangwe et al., 2023).

In a study, 10% pullulan hydrogel was formulated and assessed for its ability to cure wounds. The results demonstrated that applying the hydrogel topically quickened the healing process for wounds. They clarified that PUL's antioxidant and energy-producing qualities, which resulted in a quick healing. It was underlined that as it is a biodegradable polysaccharide polymer, it may also provide energy to cells that are actively involved in healing, such as fibroblasts. Furthermore, its hygroscopic nature promotes bacterial dehydration resulting in inactivation, and dehydration of the wound fluid may enhance the oxygenation of cells and tissues, accelerating the healing process. It was demonstrated in histological analysis that PUL-treated wounds had better fibroblast and epithelialization development. This demonstrates that PUL is a powerful substance with accelerated wound healing compared to povidine-iodine-treated (Priya et al., 2016). In excision wounds in rats, 10% PUL gel was also found to be cytocompatible and non-toxic to NIH/3T3 fibroblast cells, with quick epithelialization compared to povidone-iodine and control group, leading to an accelerated healing as a result of the collagen synthesis and remodeling (Thangavel et al., 2020).

### 2.3.3. Wound healing applications based on hyaluronic acid and pullulan

It can be seen that more effective polymer conjugates are developed by combining the advantages of polysaccharides. Various HA derivatives have been synthesized in order to modify the mechanical, rheological and swelling properties of HA, and also to adjust its degradation rate (Fallacara et al., 2018). HA based composites developed by cross-linking with various polymers and polysaccharides or by chemical synthesis have been extensively used for wound dressing applications (Graça et al., 2020). In a study, HA-graft-pullulan polymers were synthesized with different substitution degrees of HA,

and it was concluded that the films developed from these polymers resulted in a improved wound healing process (Li et al., 2018).

Wong et al. developed collagen-pullulan composites and examined their effects on cutaneous wound healing. It was reported that 5% collagen-pullulan tissue scaffolds exhibited positive properties in wound healing by ensuring cellular growth and continuity with their water retention and flexibility properties (Wong et al., 2011). It was also reported that biomimetic collagen-pullulan hydrogels increased the stem cell property and wound healing potential of adipose-derived mesenchymal stem cells (Garg et al., 2012). Rustad et al. stated that biomimetic pullulan-collagen hydrogel increased mesenchymal cell angiogenic capacity and wound healing (Rustad et al., 2012). In another study, pullulan cross-linked with trimetaphosphate was developed as a novel vascular biomaterial for smooth muscle cell proliferation (Autissier et al., 2007).

### 2.4. Main Purpose of the Study

The wound healing process is initiated after skin damage occurs with external factors such as physical, chemical, thermal, biological and so on (Qing, 2017). This process normally occurs through well-established, overlapping steps called hemostasis, inflammation, proliferation, and remodeling. Cutaneous wound healing is an essential physiological process that consists of the cooperation of many stem cells and their products (Shaw and Martin, 2009). However, prolonging the healing process and progression of an acute wound to a chronic wound are undesirable situations that can negatively affect this process, and often cause the development of scar tissue (Graça et al., 2020). Various wound care products are available on the market to accelerate and support the wound healing process, targeting both acute and chronic wounds. Wound dressing materials from these products should absorb wound extrudates, keep the wound area humid and protect the wound from infections. Many biopolymers are used solely or in combination with natural or synthetic polymers in the preparation of wound dressings (Frenkel, 2014; Priya et al., 2016; Graça et al., 2020).

Because of their high water retention capacity, hydrogels are excellent choices for wound dressings because they promote wound healing by keeping the wound moist and eliminating excess fluid (Elangwe et al., 2023). However, hydrogels constituting the

composition of wound dressings have been developed as materials with increased functionality by cross-linking natural or synthetic polymers or synthesizing graft copolymers (Priya et al., 2016; Fallacara et al., 2018). This brings about difficulties in the development and characterization of hydrogels, making physical polymer mixtures more useful. Additionally, hydrogels can retain more water than traditional dry wound dressings, which can be improved by adding additional bioactive compounds (Seiser et al., 2022).

For this purpose, gel type formulations prepared from physical mixtures of HA and PUL can improve and accelerate the wound healing proces. Because of the fact that there was no study in the literature examining the wound healing effects of non-crosslinked gel formulations based on HA and PUL binary physical mixtures constitutes the unique value of this study.

# 3. MATERIALS AND METHODS

## 3.1. Materials

The list of materials and instruments used in this study were given in Table 2 and Table 3, respectively.

**Table 2.** The materials used in the study

| Material | Supplier |
|---|---|
| Adhesive-coated slides | Marienfeld GmbH, Germany |
| Female Swiss Albino Mice | Van Yüzüncü Yıl University Experimental Medicine Research Application Center, Türkiye |
| Glycerol ≥99.0% | Emsure®, Merck Millipore, Germany |
| Hematoxylin and eosin staining solution | Sigma Aldrich, Germany |
| Hyaluronic Acid ≥95.0% | Galenik Ecza., Türkiye |
| Ketamine HCL | Atafen-Veterinary Pharmacy, Türkiye |
| Paraffin wax | Sigma Aldrich, Germany |
| Pullulan ≥90.0% | Hayashibara Co., Ltd, Japan |
| Xylazine HCL | Atafen- Veterinary Pharmacy, Türkiye |

**Table 3.** The instruments used in the study

| Device | Model |
|---|---|
| Rheometer | Hybrid Rheometer, TA Instrument, HR-Discovery, USA |
| Auto Mixer | HS-100D, Daihan Scientific, Korea |
| Deionized Water Device | MILLIPORE Direct-Q 5, Merck, Germany. |
| Digital camera | DFC490, Leica Microsystems CMS GmbH, Germany |
| Differential Scanning Calorimetry | Setaram Labsys, DSC131 Evo, France |
| DSLR Camera | EOS 300D Canon Inc., Japan |
| Electronic Balance | XB 220A, Precisa, Switzerland |
| Leica model microscope | DMI 6000B, Leica Microsystems, Germany |
| Magnetic Stirrer | MR Hei-Standard, Heidolph, Germany |
| Microtome | Waldorf, Germany |
| pH-Meter | HANNA HI2202-02 Edge®, Hanna Instruments, USA. |
| Refrigerator | KDN53NW22N, Bosch, Germany |
| Texture Analyzer with Probe (P10 Perspex) | TA-XT Plus, Stable Micro Systems, United Kingdom |

### 3.2. Methods

#### 3.2.1. Formulation approach for the development of gels

The analysis of experimental design and calculation of predicted data were performed using Design Expert software Design-Expert 11.0.0 program (Stat-Ease Inc.; United States). A Design of Experiments (DOE) matrix was generated based on early experimental results, to identify the ideal concentrations of key constituents. Hyaluronic acid (HA), pullulan (PUL), and glycerol (GLY) ratios were chosen as the independent variables in this design for the gel compositions. The parameters including strength (firmness), spreadability, adhesive force and adhesiveness of the gel formulations that were obtained with Texture profile analysis (TA) at a temperature of 25°C were used as the dependent variables.

Table 4 provides the variables of the Box-Behnken Experimental Design (BBED) matrix. Within the DOE matrix, the software produced a total of 17 alternative formulations, including 12 unique formulations and 5 replications of the center point formulation. Three levels of each independent variable were being evaluated at: high, medium, and low. According to Table 5, the maximum and minimum values of each parameter under consideration in this system were marked as (-1) and (+1), which represented the minimum and maximum value, respectively.

**Table 4.** Variables of the BBED Matrix

| **Variables and constraints in BBED** | | |
|---|---|---|
| Factors | Level of the variables | |
| Indipendent variables | Low (-1) | High (+1) |
| $X_1$=Hyaluronic acid (%) | 2.00 | 5.00 |
| $X_2$=Pullulan (%) | 2.00 | 8.00 |
| $X_3$=Glycerol (%) | 0.00 | 1.00 |
| **Dependent variables** | **Constrains** | |
| $Y_1$= Firmness (g) | Minimize | |
| $Y_2$= Adhesive force (g) | Minimize | |
| $Y_3$= Spreadability (g.sec) | Minimize | |
| $Y_4$= Adhesiveness (g.sec) | Minimize | |

#### 3.2.2. Gel preparation

To prepare the gel formulations, HA at various concentrations was dispersed in preheated distilled water containing GLY at various concentrations at 50 ˚C in a glass

beaker with a slow addition, and stirred at 600 rpm using a overhead stirrer (HS-100D, Daihan Scientific, Korea). After a homogenous dispersion obtained, PUL at various amounts added to the obtained solution, and then it was cooled down to room temperature. Subsequently, a clear and transparent gel was obtained (Tuncay Tanrıverdi et al., 2018).

### 3.2.3. Texture profile analysis

Texture profile analysis (TA) of the gel formulations was investigated using a TA XT plus Texture Analyser (Stable Microsystems, USA) in compression mode using a cone-cap assembly. The instrument was calibrated for force and distance measurement at room temperature with a 5 N load cell. The 45° cap was partly filled with 1 g of sample and set on the platform of the analyzer prior to profiling. A corresponding 45° cone was used to detect dynamics of spreading and retracting forces as it moved vertically toward the bottom of the cap followed by withdrawal to its original point. The cone and cap assembly were aligned coaxially. During the test, the probe proceeded to penetrate the sample (i.e., compression mode) at a test speed of 2 mm/s to a depth until it reached the distance of 1 mm from the bottom of the cap with a trigger force of 10 g. This was immediately followed by an upward movement of the probe (i.e., retraction mode) at a speed of 10 mm/s. Three replicate analyses were performed at room temperature for each sample, providing the same conditions for each measurement. Exponent software *v.6.1.27.0* (Stable Microsystems, USA) *was used* to collect the data and generate a curve plotted as load (g) vs. time (sec). Parameters of gel such as firmness, spreadability, adhesive force and adhesiveness were determined from the graph "force-time". A maximum force value on the obtained graphs is a measure of the firmness (g) of the sample at the specified depth. The area under the positive curve is indicated as spreadability (g.sec). The adhesive force (g) is the negative peak value and adhesiveness is the area under the negative curve (g.sec) (Bogdan et al., 2016; Maslii et al., 2020). The experimental setup used for TA study was shown in Figure 4.

**Figure 4.** The experimental setup used for Texture Profile Analysis study.

### 3.2.4. Data analysis and experimental design optimization studies

The Design Expert software examined the experimental design and produced 3D response surface graphs using polynomial equations, and ANOVA analysis was used to determine the best model for each response parameter. The ideal composition within the stated design range might be found by applying the "desirability function" method in accordance with limitations listed in Table 4. The optimal composition for the gel formulations was determined by computer calculations, with the greatest desirability values chosen at random. The experimental results were compared with the expected values to confirm consistency.

### 3.2.5. Further examination of optimized gel formulations

#### pH measurement of the optimized gel formulations

The pH of gels was determined using HANNA HI2202-02 Edge® pH-meter with a glass electrode (Hanna Instruments, USA). The measurements were made in triplicate and data were given as mean ±SD.

**Differential scanning calorimetry analysis**

The differential scanning calorimetry (DSC) analysis of HA and PUL, physical mixture of HA and PUL as well as gel formulations (F1, F3 and F4) were carried out with DSC (Setaram Labsys, DSC131 Evo, France) under a constant flow of argon gas with a flow rate of 100 mL $min^{-1}$. The samples of amount of 5-10 mg were weighted through an analytical balance (MT MS 105, Mettler Toledo, USA), the aluminum pans sealed hermetically, then heated at a rate of 10 °C $min^{-1}$ from 25 °C to 250°C, and an empty pan was used as reference (Mendonsa et al., 2018; Pan et al., 2020; Singh et al., 2021).

**Rheological evaluation of the optimized gel formulations**

A TA Discovery HR-1 hybrid rheometer (TA Instruments, USA) was employed to perform rheological assessments on six chosen formulations. Measurements were conducted at both 25°C and 32°C using a temperature-controlled Peltier plate, and a Smart Swap TM parallel steel plate geometry with a 500 μm gap was utilized. Shear rates were varied within the range of 10-1000 1/s during the experiment. Prior to each trial, each sample was placed in the sample holder and allowed to equilibrate to a stable temperature for approximately 5 minutes (Bektas et al., 2020; Rençber and Karavana, 2020).

**3.2.6. *In vivo* experiments**

**Animals**

Female Swiss mice (20-25 g) were provied by Van Yüzüncü Yıl University Experimental Medicine Research Application Center. All animals were housed in a well-ventilated room with 12-h light/dark cycles at 22 ± 1 ˚C and allowed free access to food and water *ad libitum*. The animal study was approved by the Local Ethics Committee of Van Yüzüncü Yıl University (Approval Number: 2021/12-17). Animal care and research protocols were based on the principles and guidelines adopted by the Guide for the Care and Use of Laboratory Animals (NIH publication No: 85–23, revised in 1985) (Bektas et al., 2020).

The animals were divided into 7 groups including 7 animals per group as follows: Negative Control, Vehicle (GLY 1% w/w in distilled water), F1 (HA/GLY 2/1%, w/w), F2 (HA/PUL/GLY 2/2/1%, w/w/w), F3 (HA/PUL/GLY 2/5/1%, w/w/w), F4 (HA/PUL/GLY 2/8/1%, w/w/w), and Reference (Madecassol®).

**Circular excision wound model**

Combination of ketamine HCl (100 mg/kg) and xylazine HCl (10 mg/kg) was administered to the mice intraperitoneally for anesthesia. Then, circular excision wounds were formed in mice under anesthesia by using biopsy punch with a diameter of 6 mm, and agents as described in animals section were applied externally to the wounds once a day for 12 days (Sadaf et al., 2006). Photographs of the wound areas were taken every other day with a digital camera (Canon EOS 300D, USA), and the area of the wound areas was calculated using the ImageJ program (Akkol et al., 2011). In the circular excision wound model, the following formula was used to calculate the percentage of contraction rates:

$$\text{Contraction}(\%) = \frac{V - T}{V} x100$$

V: Measured wound area of the vehicle group ($mm^2$)

T: Measured wound area of the test group ($mm^2$)

**Histological procedures**

On the 12$^{th}$ day of the experiment, the skin tissues from wound areas were excised carefully using fine scissors and forceps, and immediately fixed in 10% neutral buffered formalin for 48 h at 4 °C. Following washing the samples with phosphate buffered saline (pH: 7.4), a graduated ethanol series was used to dehydrate the tissues. Next, the tissues were embedded in paraffin wax. The tissue sections (5 µm thick) were taken from paraffin blocks using a MICROM HM 325 manual microtome (Waldorf, Germany), and then the sections were put onto adhesive-coated slides (Marienfeld GmbH, Germany). Following deparaffinization and rehydration, the sections were stained with hematoxylin and eosin (H&E). The preparations were examined for histopathology using a Leica DMI 6000B model microscope (Leica Microsystems, Wetzlar, Germany), and photographs were taken

using a Leica Digital DFC490 model camera (Leica Microsystems CMS GmbH, Germany) that was attached to the microscope.

The histopathological examination of the skin tissues were performed to assess the principal events during wound healing including scab and formation of ulcus on the wound surface, re-epithelization (regeneration of epidermis); infiltration of dermal inflammatory cells, fibroblast proliferation, regeneration of collagen fiber, and neovascularization in the dermis using the following semi-quantitative scoring system: none (–), (+) mild, (++) moderate, (+++) severe (Oz et al., 2016).

### 3.2.7. Statistical analysis

The Shapiro-Wilk test was carried out to evaluate whether the data set obtained from the groups is normally distributed. Then, one-way analysis of variance (ANOVA) and Dunnett's post hoc test was performed, and all groups were compared to the vehicle group. Additionally, negative control group was compared to the vehicle group by Student's t test. Statistical significance was determined by comparing all groups to the control group, with a significance level of $p<0.05$.

# 4. RESULTS

## 4.1. Assessment of the Box-Behnken Experimental Design

Table 5 provides an overview of 17 formulations of their variables, constrains and corresponding responses of them, which were generated using the Design Expert 11.0.0 software (Stat Ease, USA) within the BBED matrix corresponding to Table 4. Also, Table 6 demonstrates the regression equations of fitted models of the BBED Matrix. The data obtained from TA study used for developing the matrix, in which Y1, Y2, Y3 and Y4 stands for Firmness (g), Adhesive force (g), Y3= Spreadability (g.sec), and Y4= Adhesiveness (g.sec), respectively.

**Table 5.** Responses of the BBED Matrix

| | **Factors** | | | **Responses** | | | |
|---|---|---|---|---|---|---|---|
| **Batch No** | **$X_1$** | **$X_2$** | **$X_3$** | **$Y_1$** | **$Y_2$** | **$Y_3$** | **$Y_4$** |
| 1 | 8 | 5 | 0 | 1348.22 | 77.57 | 876.45 | 44.78 |
| 2 | 8 | 8 | 0.5 | 1361.65 | 84.15 | 912.21 | 95.27 |
| 3 | 5 | 5 | 0.5 | 387.10 | 97.75 | 242.83 | 136.22 |
| 4 | 2 | 5 | 0 | 126.51 | 78.58 | 66.61 | 16.80 |
| 5 | 5 | 8 | 0 | 724.87 | 105.20 | 465.38 | 150.27 |
| 6 | 8 | 5 | 1 | 1308.46 | 98.40 | 920.92 | 189.09 |
| 7 | 2 | 5 | 1 | 123.67 | 73.98 | 72.652 | 24.67 |
| 8 | 2 | 8 | 0.5 | 151.43 | 70.15 | 89.83 | 24.80 |
| 9 | 5 | 2 | 0 | 1019.31 | 72.53 | 737.96 | 105.22 |
| 10 | 2 | 2 | 0.5 | 137.54 | 73.16 | 82.90 | 19.81 |
| 11 | 5 | 2 | 1 | 546.77 | 87.66 | 371.78 | 79.64 |
| 12 | 5 | 5 | 0.5 | 493.37 | 97.46 | 294.31 | 82.26 |
| 13 | 5 | 8 | 1 | 637.04 | 90.42 | 407.16 | 137.17 |
| 14 | 5 | 5 | 0.5 | 643.14 | 88.94 | 381.53 | 126.76 |
| 15 | 8 | 2 | 0.5 | 915.45 | 81.67 | 699.30 | 113.88 |
| 16 | 5 | 5 | 0.5 | 570.24 | 84.73 | 369.79 | 145.94 |
| 17 | 5 | 5 | 0.5 | 608.82 | 88.872 | 444.03 | 166.12 |

**Table 6.** Regression equations of fitted models of the BBED Matrix

| **Regression equations of fitted models** | |
|---|---|
| $\boldsymbol{Y1}$=635.15-549.33$X_1$+31.99$X_2$-75.37$X_3$ | (Eq.1) |
| $\boldsymbol{Y2}$ =91.55+5.74$X_1$+4.36$X_2$+2.07$X_3$+1.37$X_1X_2$+6.36 $X_1X_3$-7.48$X_2X_3$-10.54$X_1^2$-3.78$X_2^2$+1.13$X_3^2$ | (Eq.2) |
| $\boldsymbol{Y3}$=437.39+387.11$X_1$-2.17$X_2$-46.74$X_3$ | (Eq.3) |
| $\boldsymbol{Y4}$=131.46+44.62$X_1$+11.12$X_2$+14.19$X_3$-5.90$X_1X_2$+34.11$X_1X_3$+3.12$X_2X_3$-58.63$X_1^2$-9.39$X_2^2$-4.00$X_3^2$ | (Eq.4) |

Figures 5, 6, 7 and 8 demonstrate the 3D surface plot graphs of the relationship between independent variables and firmness, adhesive force, spreadability and adhesiveness response, respectively.

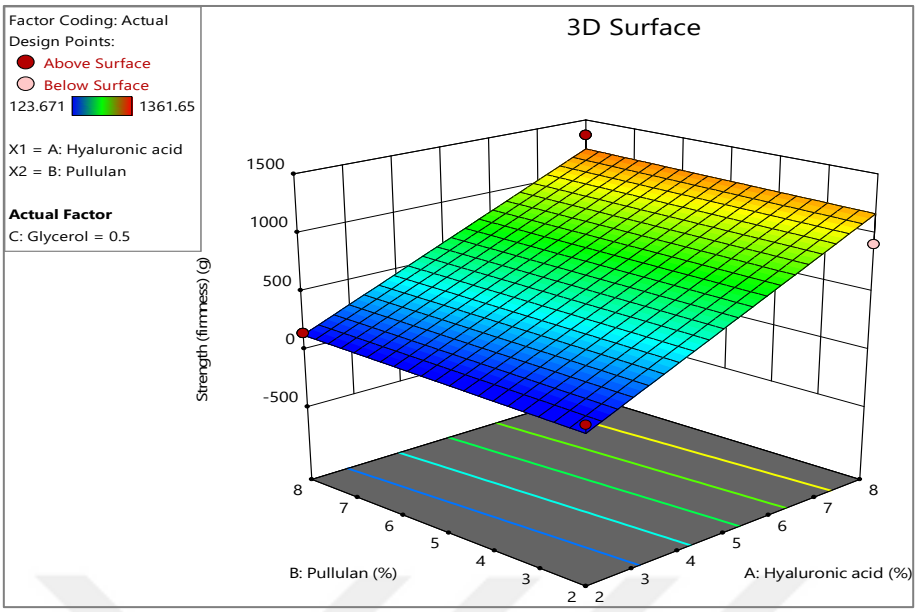


**Figure 5.** 3D surface plot representation of the relationship between independent variables and firmness response.

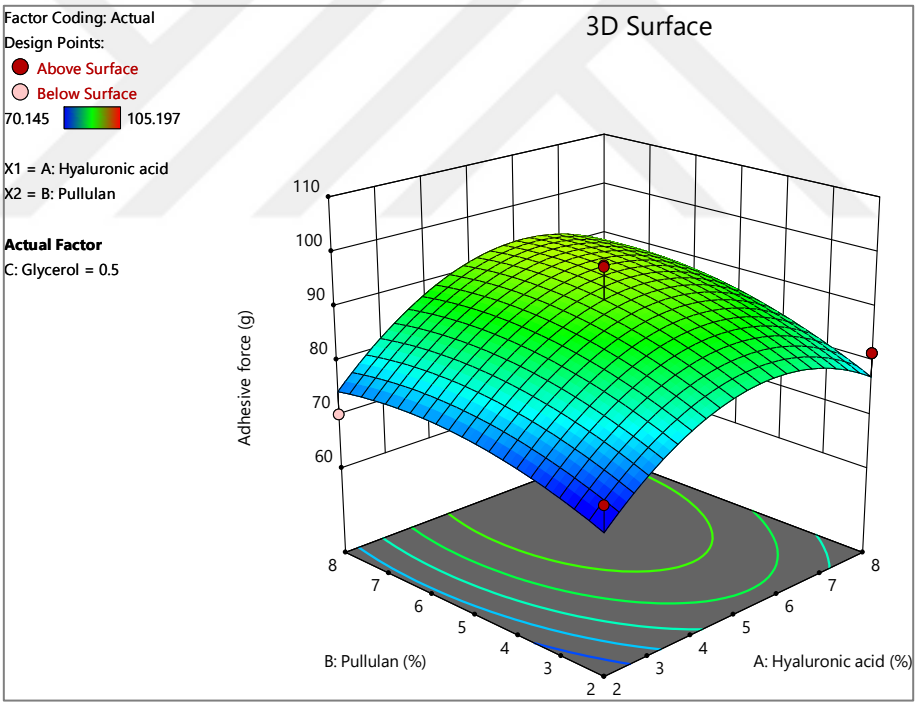


**Figure 6.** 3D surface plot representation of the relationship between independent variables and adhesive force response.

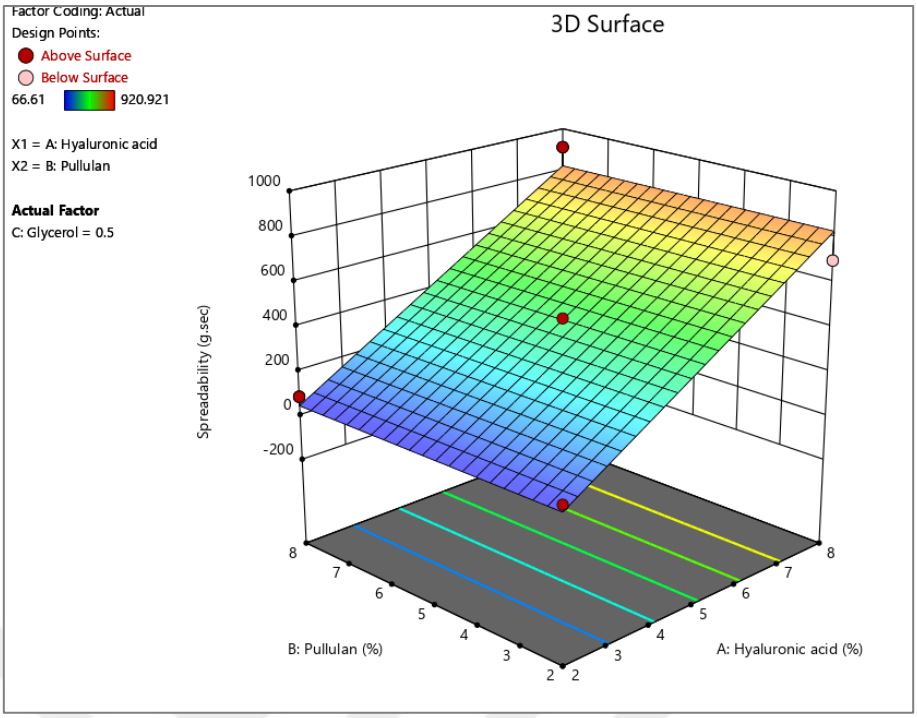


**Figure 7.** 3D surface plot representation of the relationship between independent variables and spreadability response.

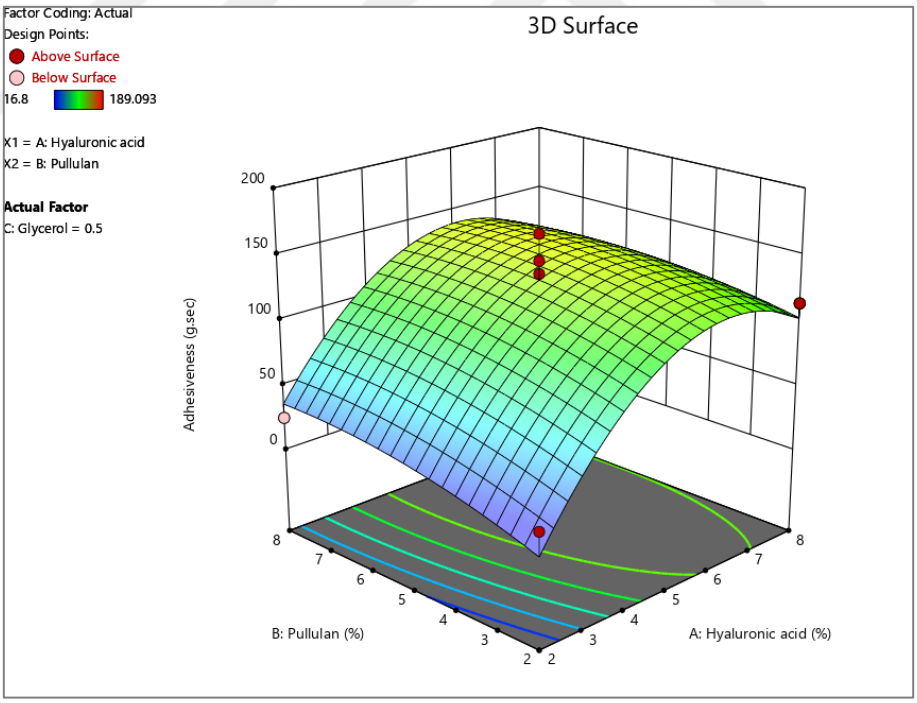


**Figure 8.** 3D surface plot representation of the relationship between independent variables and adhesiveness response.

### 4.2. Texture Analysis Data Obtained with Selected Formulations

TA plot obtained for F1-6 using a cone-cap probe. The data were plotted as force (g) vs. time (sec)., and calculated values were shown in Figs. 9-14.

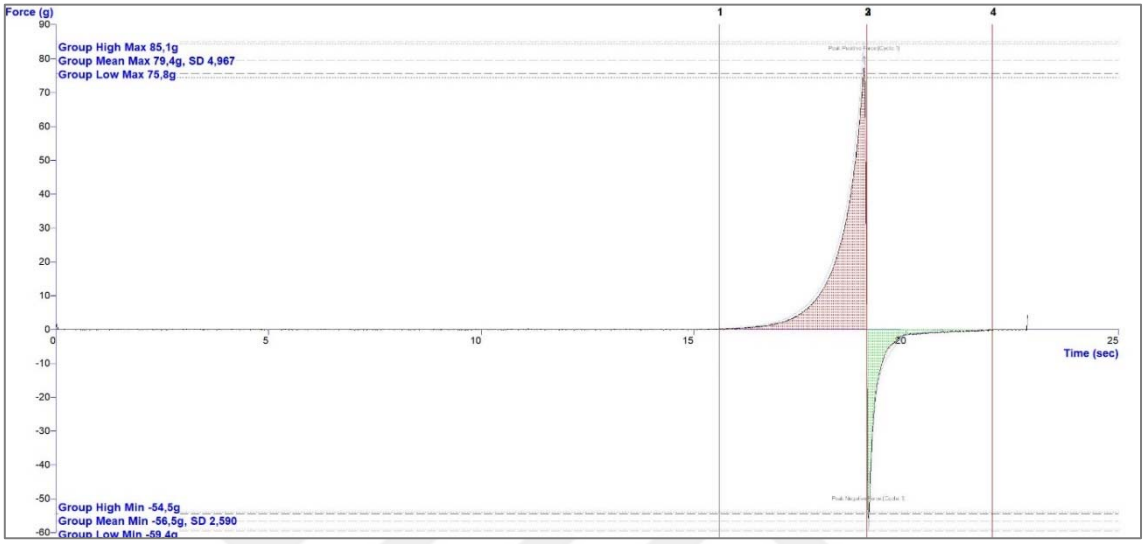


**Figure 9.** TA plot obtained for F1 using a cone-cap probe. The data were plotted as as force (g) vs. time (sec).

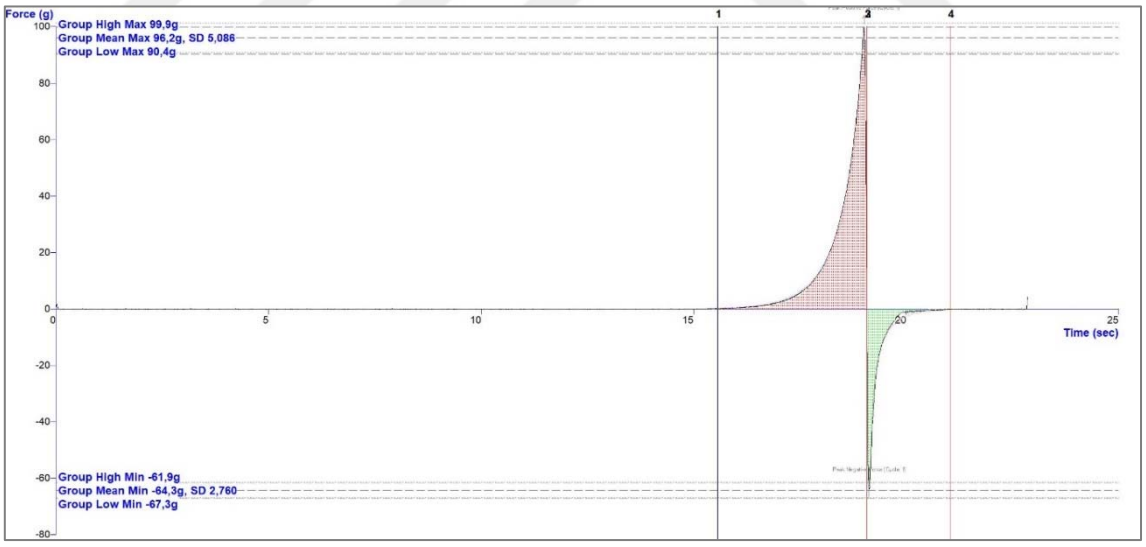


**Figure 10.** TA plot obtained for F2 using a cone-cap probe. The data were plotted as as force (g) vs. time (sec).

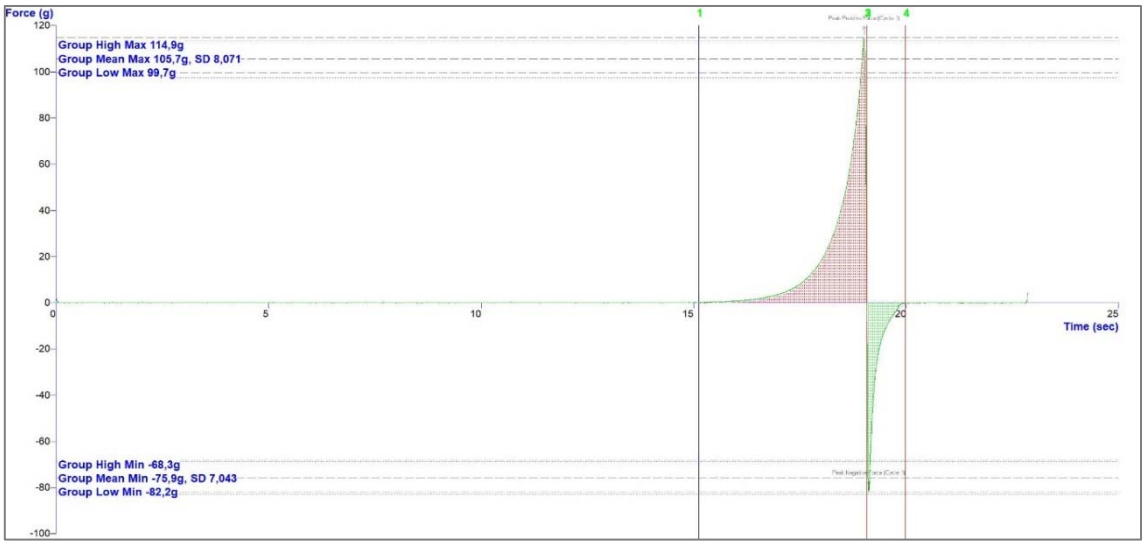


**Figure 11.** TA plot obtained for F3 using a cone-cap probe. The data were plotted as as force (g) vs. time (sec).

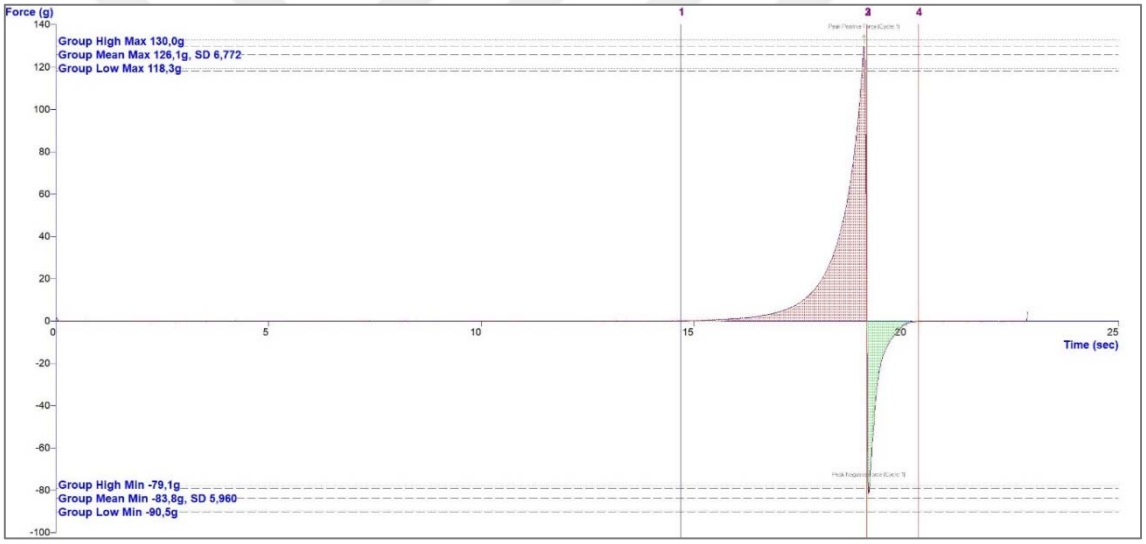


**Figure 12.** TA plot obtained for F4 using a cone-cap probe. The data were plotted as as force (g) vs. time (sec).

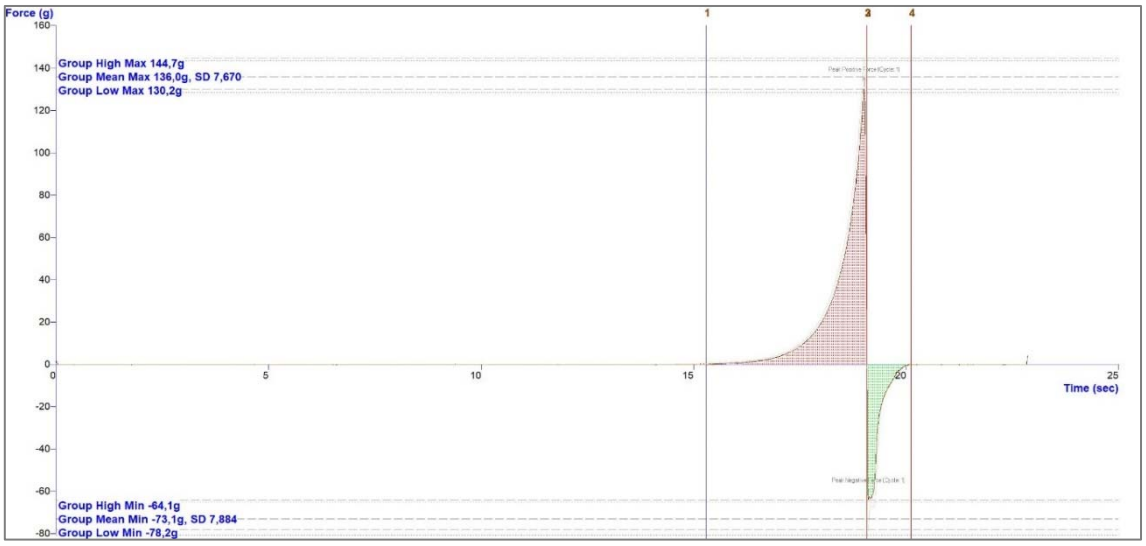


**Figure 13.** TA plot obtained for F5 using a cone-cap probe. The data are plotted as as force (g) vs. time (sec).

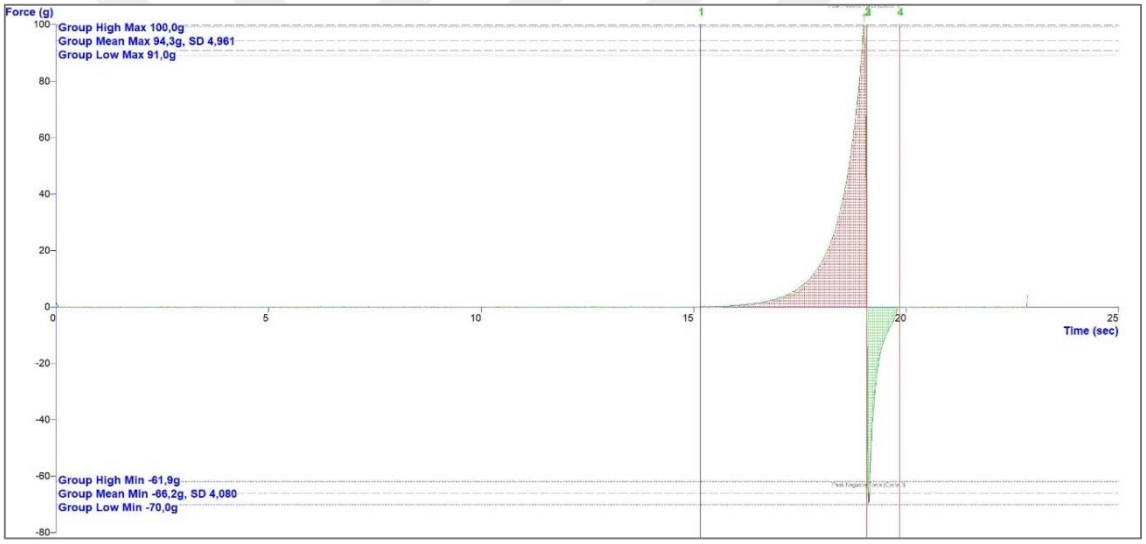


**Figure 14.** TA plot obtained for F6 using a cone-cap probe. The data are plotted as force (g) vs. time (sec).

### 4.3. Validation of the model employed with selected formulations

As a result of the analyses conducted using the BBED, the validation of model employed was carried out with selected formulations, as indicated by the data obtained from the TA study, which were shown Table 7.

**Table 7.** Validation of the model employed with selected formulations

| Num. | Formulation Codes | X1=Hya (%) | X2=Pul (%) | X3=Gly (%) | *Y1= Firmness (g)* | Y2= Adhesive force (g) | Y3= Spreadability (g.sec) | Y4= Adhesiveness (g.sec) | Desirability value |
|---|---|---|---|---|---|---|---|---|---|
| **Ref*** | **F1** | **2** | **0** | **1** | 79,394 ± 4,967 | 56,541 ± 2,590 | 44,323 ± 3,937 | 12,970 ± 1,448 | **-** |
| 84 | F2 | 2.00 | 2.00 | 1 | 96,159 ± 5,086 | 64,333 ± 2,760 | 53,934 ± 2,285 | 15,099 ± 0,390 | 0.99 |
| 90 | F3 | 2.00 | 5.00 | 1 | 105,684 ± 8,071 | 75,911 ± 7,043 | 60,088 ± 6,842 | 16,300 ± 0,965 | 0.99 |
| 11 | F4 | 2.00 | 8.00 | 1 | 126,077 ± 6,772 | 83,834 ± 5,960 | 71,923 ± 6,160 | 19,618 ± 1,738 | 1 |
| 1 | F5 | 2.00 | 7.00 | 1 | 135,996 ± 7,670 | 73,141 ± 7,884 | 78,549 ± 5,291 | 21,479 ± 1,644 | 0.99 |
| 98 | F6 | 2.00 | 2.00 | 0.15 | 94,290 ± 4,961 | 66,188 ± 4,080 | 53,806 ± 4,463 | 13,614 ± 1,307 | 0.99 |

*F1: without pullulan.

### 4.4. Further examination of the optimized gel formulations

#### 4.4.1. pH measurement of the optimized gel formulations

The pH measurements for the six optimal gel formulations were 6.40 ±0.13, 6.67 ± 0.04, 6.75 ± 0.05, 6.55 ± 0.03, 6.76 ± 0.03, and 6.69 ± 0.16, respectively.

#### 4.4.2. Differential scanning calorimetry analysis

The thermograms of HA and PUL, physical mixture of HA and PUL as well as gel formulations (F1, F3 and F4) obtained from DSC analysis were demonstrated in Figure 15.

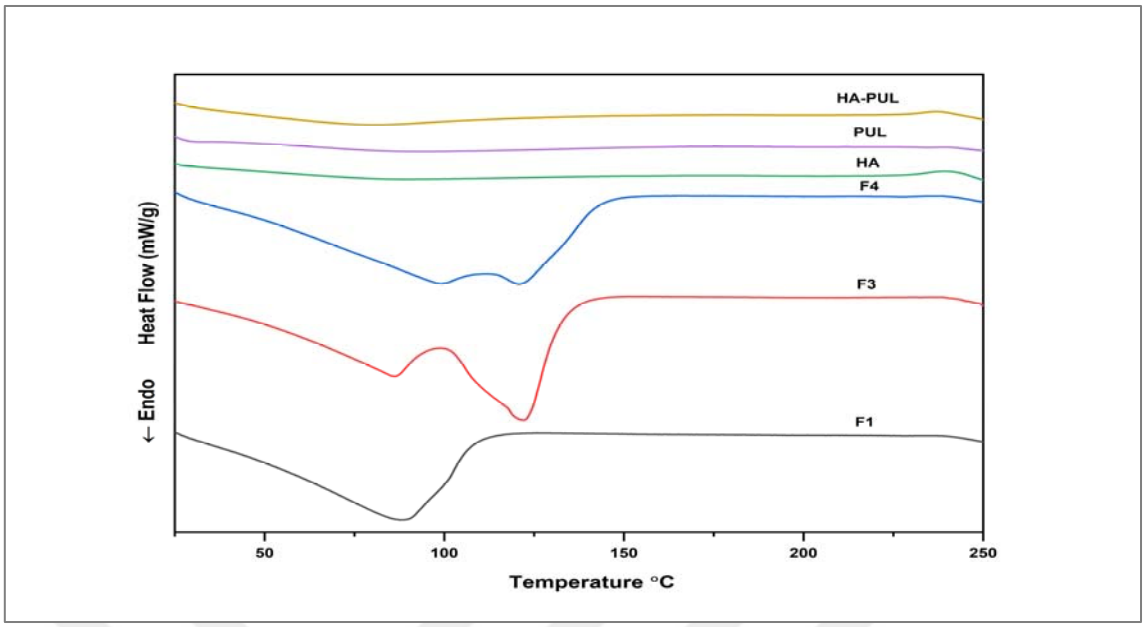


**Figure 15.** Differential scanning calorimetric thermograms of the HA and PUL, physical mixture of HA and PUL and gel formulations (F1, F3 and F4).

**Abbreviations:** HA: Hyaluronic acid; PUL: Pullulan; HA-PUL: Physical mixture of hyaluronic acid and pullulan; F1: HA, PUL and GLY (2/0/1%, w/w/w) gel formulation; F2: HA, PUL and GLY (2/5/1%, w/w/w) gel formulation; F4: HA, PUL and GLY (2/8/1%, w/w/w) gel formulation.

### 4.4.3. Rheological Evaluation of the Optimized Gel Formulations

Flow curves depicting viscosity as a function of shear rate and shear stress as a function of shear rate were shown in Figure 16-19.

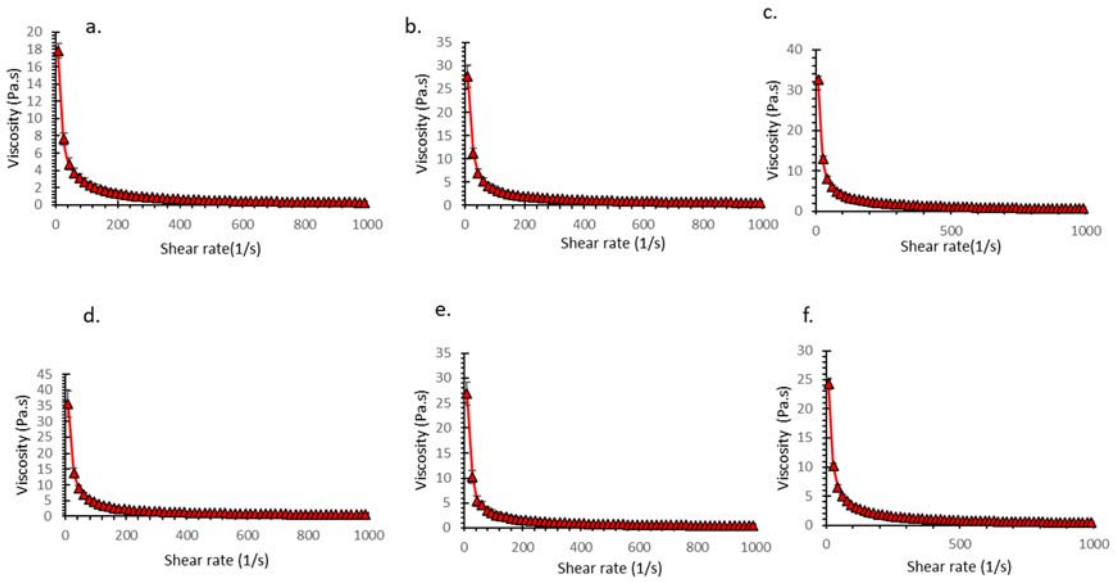


**Figure 16.** Viscosity changes over shear rate of a. F1; b. F2; c. F3; d. F4; e. F5; and f. F6 formulations at 25ºC.

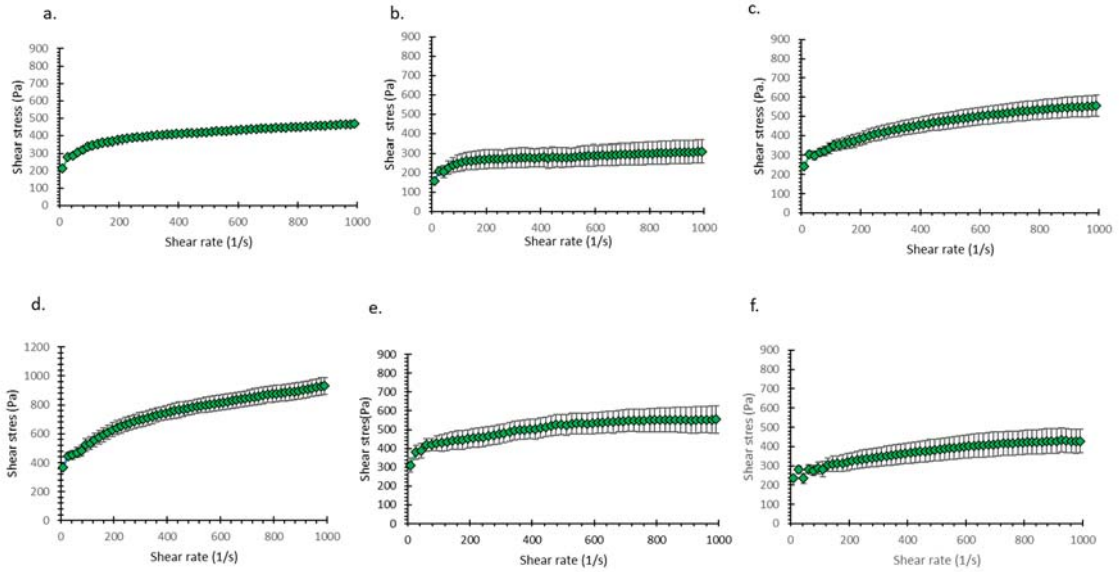


**Figure 17.** Flow curves of a. F1; b. F2; c. F3; d. F4; e. F5; and f. F6 formulations at 25ºC.

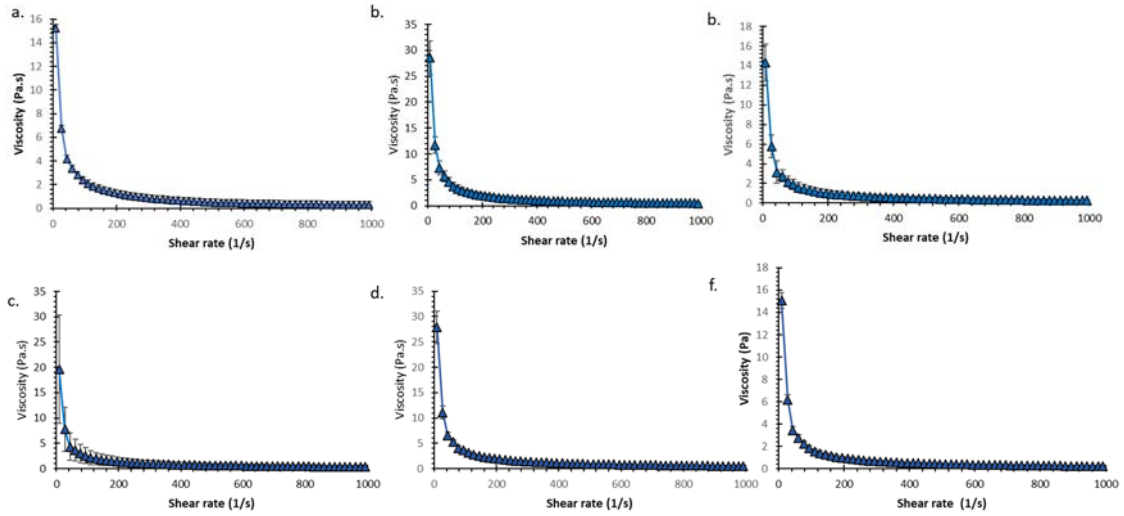


**Figure 18.** Viscosity changes over shear rate of formulations a. F1; b. F2; c. F3; d. F4; e. F5; and f. F6 formulations at 32ºC.

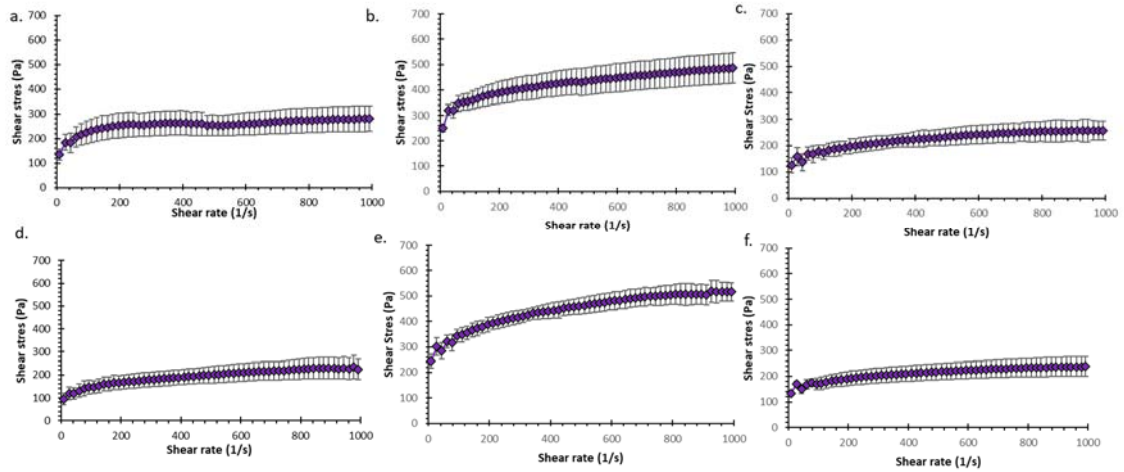


**Figure 19.** Flow curves of a. F1; b. F2; c. F3; d. F4; e. F5; and f. F6 formulations at 32ºC.

### 4.4.4. *In Vivo* experiments

#### Investigation of healing effect on circular excision wound model

The percentage contraction effect of the applied agents on the area of circular excision wound model in mice for 12 days were given in Table 8 and Figure 20.

**Table 8.** The percentage contraction effects of the applied agents on the area of circular excision wound model in mice

| Groups | Day 0 | Day 2 | Day 4 | Day 6 | Day 8 | Day 10 | Day 12 |
|---|---|---|---|---|---|---|---|
| **Negative Control** | 32.29 ± 1.34 | 29.02 ± 0.66 | 25.68 ± 3.08 | 15.19 ± 2.34 | 11.19 ± 2.17 | 6.07 ± 0.41 | 4.39 ± 0.73 |
| **Vehicle** | 31.98 ± 3.42 | 29.30 ± 3.12 | 23.10 ± 3.91 | 17.50 ± 1.97 | 14.02 ± 1.44 | 8.52 ± 1.93 | 5.86 ± 0.62 |
| **F1** | 32.34 ± 2.65 | 31.66 ± 3.68 | 26.85 ± 3.58 | 21.88 ± 2.56 | 13.72 ± 1.26 (2.1) | 8.50 ± 1.57 (0.23) | 4.07 ± 0.66 (30.5) |
| **F2** | 31.41 ± 1.51 | 29.17 ± 3.84 (0.44) | 21.87 ± 2.64 (5.3) | 14.88 ± 1.04 (14.9) | 9.65 ± 1.06 (31.2) | 7.67 ± 0.58 (9.9) | 4.32 ± 0.44 (26.2) |
| **F3** | 32.60 ± 1.59 | 29.82 ± 1.33 | 20.47 ± 0.93 (11.4) | 13.17 ± 0.61 (24.7) | 6.74 ± 1.35 **(51.9)**** | 3.41 ± 0.65 **(59.9)**** | 0.39 ± 0.12 **(91.1)***** |
| **F4** | 32.47 ± 2.71 | 30.40 ± 2.34 | 20.06 ± 2.25 (13.2) | 9.500 ± 1.17 **(54.3)**** | 5.27 ± 0.73 **(62.4)***** | 1.07 ± 0.27 **(87.4)***** | 0.16 ± 0.10 **(97.3)***** |
| **Reference (Madecassol®)** | 32.62 ± 3.06 | 29.55 ± 1.99 | 21.27 ± 8.88 (7.9) | 14.64 ± 0.62 (16.3) | 9.12 ± 1.37 (34.9) | 4.43 ± 0.81 **(48.0)*** | 2.38 ± 0.95 **(59.4)**** |

The values are expressed as Mean ± S.E.M. (%Contraction).

*: p<0,05; **: p<0,01; ***: p<0,001; ****: p<0,0001

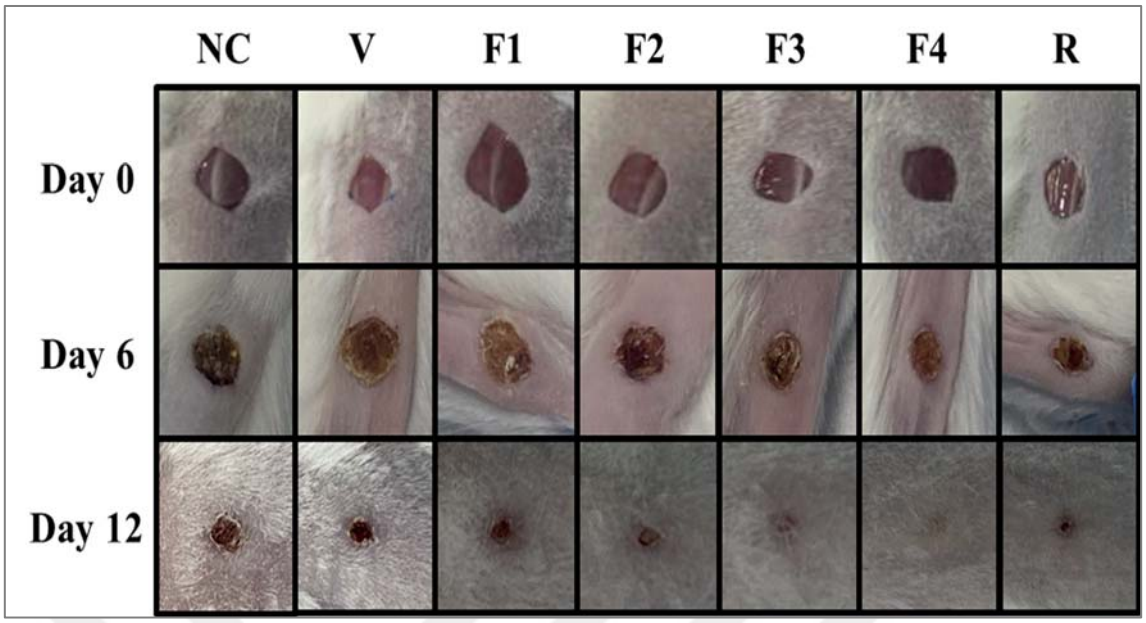


**Figure 20.** The images of circular excision wounds at different days.

**Histological evaluation of wound healing activity**

Scoring of histopathological lesions in the skin tissues from wound areas of different experimental groups were summarized in Table 9. The representative microscopic photographs were also demonstrated for each experimental group in Figure 21.

**Table 9.** Scoring of the histopathological findings in the skin sections of the different experimental groups.

| *Alteration* / *Groups* | *Scab* | *Ulcus* | *Re-epithelization* | *Infiltration of inflammatory cells* | *İncrease in the number of fibroblasts* | *Regeneration of collagen fibers* | *Neovascularization* |
|---|---|---|---|---|---|---|---|
| Neg. Control | +++ | +++ | – | ++/+++ | –/+ | –/+ | – |
| Vehicle Con. | ++ | +/++ | + | ++ | + | + | + |
| Reference | ++ | ++ | + | ++/+++ | –/+ | –/+ | –/+ |
| F1 | ++/+++ | ++/+++ | – | ++/+++ | –/+ | –/+ | –/+ |
| F2 | +++ | +++ | – | +++ | –/+ | –/+ | – |
| F3 | –/+ | – | +++ | + | + | + | + |
| F4 | ++ | ++ | + | +/++ | –/+ | –/+ | –/+ |

Scores; (–) none, (+) mild, (++) moderate, (+++) severe.

According to the histological examinations of wound sections of negative control group including untreated animals on the 12th day of the experiment, presence of a thick scab and severe ulcus formation were observed on the wound surface. The absence of re-

epithelization (regeneration of epidermis) and existence of intense inflammatory cells in the granulation tissue of the wound bed were noted. The proliferation of fibroblasts, formation of collagen fibers was poorly detected and neovascularization were not determined in the dermis of wound bed. Those findings indicate that the healing has not been completed in this group (Figure 21A).

The vehicle group exhibited a moderate degree of scab and ulcus formation (mild to moderate) on the wound surface. The presence of a mild degree of re-epithelization were detected. Moderate infiltration of inflammatory cells in the granulation tissue of the wound bed were found. Slight increases in the proliferation of fibroblast, the regeneration of collagen fibers and the formation of neovascularization were observed. Indicating that healing activity were limited in this group (Figure 21B).

In the reference group, the presence of scab was observed moderately on the wound surface. A mild re-epithelization was detected. Moderate to severe inflammatory cell infiltration were observed in the granulation tissue of the wound bed. The proliferation of fibroblast, the regeneration of collagen fibers and the formation of neovascularization were observed poorly in the dermis of wound bed (Figure 21C). This group demonstrated better wound healing activity than negative control group.

Both of F1 and F2 groups exhibited incomplete healing in wound area, which were similar to the negative control group. A thick scab and severe ulcus formation on the wound surface were found. The re-epithelization was not formed on the wound surface. Intensive infiltration of inflammatory cells in the granulation tissue of the wound bed was detected. Poor development of the fibroblast proliferation, the collagen fiber regeneration, and the neovascularization was seen in the granulation tissue of the wound bed (Figures 21D, E).

In the F3 group, the presence of a thin scab on the well regenerated epidermis displaying keratinization was detected. No ulcus formation was determined on the wound surface and a completed re-epithelization was observed in this group. Additionally, inflammatory cells showed marked decrease when comparing negative control and other groups. Moreover, mild increases were found in the existence of the fibroblasts, amount of the collagen fibers and the formation of neovascularization in the granulation tissue of

the wound bed (Figure 21F). Based on the histopathological evaluations, formulation used in this group were determined to be more effective for wound healing that it provided a better reorganization in the wounded skin tissue.

The F4 group exhibited similar histological properties to the reference group that moderate scab and ulcus formation, a mild re-epithelization, mild to moderate Inflammatory cell infiltration, and poor improvements in terms of fibroblast proliferation, the collagen fiber regeneration and the neovascularization were determined in the wound area (Figure 21G).

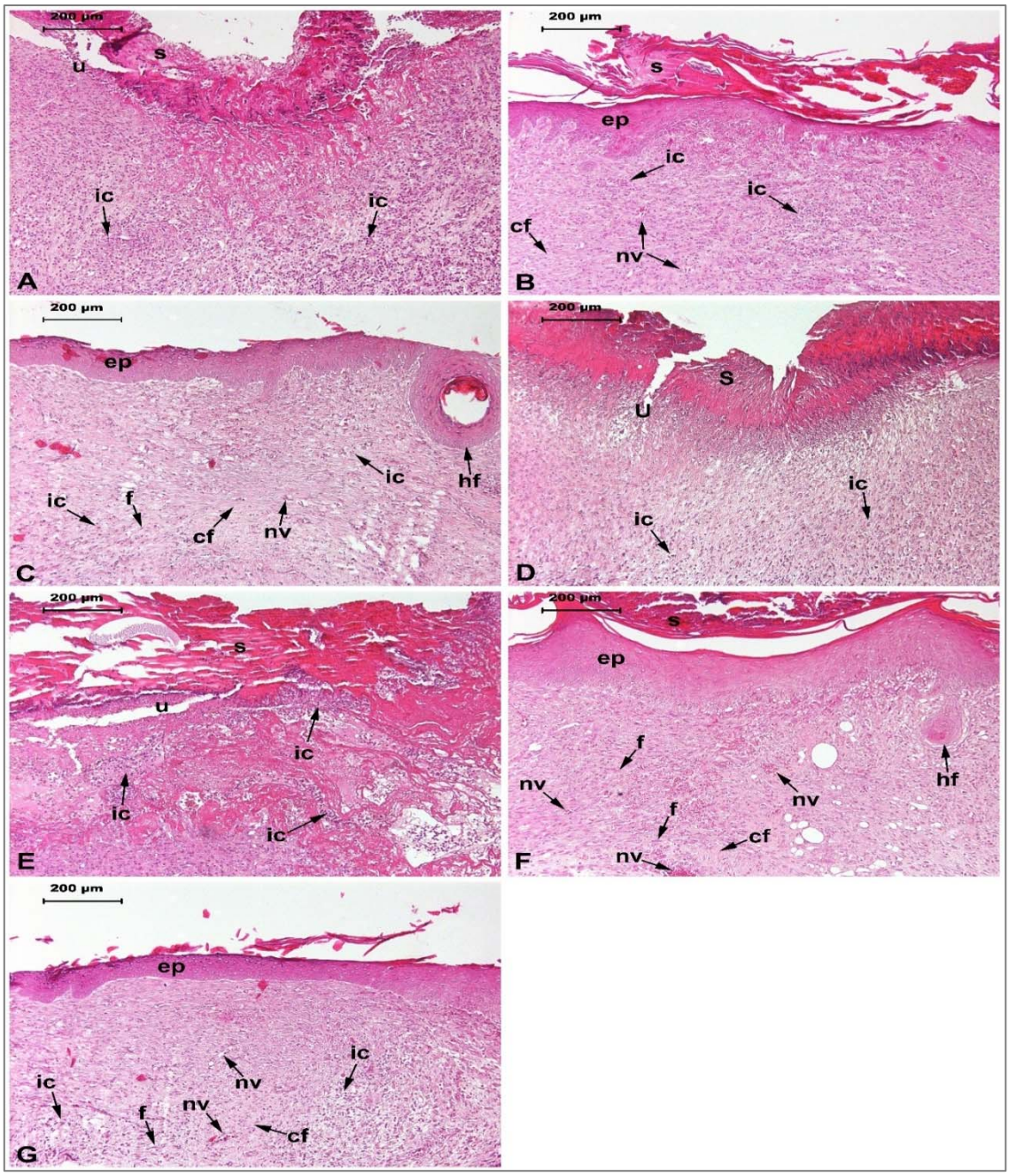


**Figure 21.** The representative photomicrographs of the skin from wound areas in the experimental groups on the 12th day.

A: negative control group, B: vehicle control group, C: reference group, D: F1 group, E: F2 group, F: F3 group, and G: F4 group. Arrows indicate events during wound healing; s: scab, u: ulcus, ic: inflammatory cells, ep: epidermis, f: fibroblast, cf: collagen fiber, nv: neovascularization (H&E, 100×).

# 5. DISCUSSION AND CONCLUSION

## 5.1. Texture Profile Analysis Study and Assessment of the Box-Behnken Experimental Design

In our study, we employed statistical parameters including R2, Adjusted R2, Pre-R2, and p-value (with a significance level of $p<0.05$) as provided by the Design-Expert® software. These parameters guided our selection of a fitted polynomial equation (Table 6) to describe the intricate connection between critical effects and interaction factors. Within these equations, the coefficients not only signify primary effects but also reveal whether they collaborate synergistically or oppose each other in influencing the response a valuable insight for our research.

Gels play a critical role in wound healing by creating a moist, protective microenvironment that facilitates tissue repair and reduces the risk of infection (Boateng et al., 2008). Consequently, the gel structure should establish a microgel network capable of withstanding physiological stresses while ensuring prolonged contact at the wound site indicating the importance of specific mechanical properties in the formulation of effective topical products for wound treatment (Firlar et al., 2022). These attributes aid in the seamless extraction of the product from its container and its application to the skin (Borzacchiello et al., 2015).

Furthermore, the textural properties of the formulations, including firmness, spreadability, adhesive forece and adhesiveness, reveal the flowable nature and deformability of the samples. The high spreadability of a gel is demonstrated by its outward flow at a 45˚ angle during the test, indicating the firmness and energy required to deform the sample to a defined depth at a temperature of 25˚C. A higher peak load and hardness work done value imply a less spreadable sample, whereas a lower peak load and hardness work done value suggest a more spreadable sample (Bogdan et al., 2020; Maslii et al., 2020). Based on these facts, the goal for a successful topical gel formulation is a quick spreading ability, which is especially important for dermatological products as it ensures effective coverage of the skin. As also observed in this study, the samples which

had a more liquid texture demonstrated a decrease in adhesiveness, as also observed in the rheological experiments (Figures 9-14).

The statistical analysis highlights the significant impact of HA concentration (X1) on firmness esponse (Y1) ($p<0,0.05$; Table 5-6, Eq. 1). The plots in Figure 5 showed a clear correlation—increased HA concentration resulted in higher firmness. Firmness was intricately linked to both HA concentration and crosslinking extent. Decreased crosslinking spacing strengthens the overall matrix and yields a firmer gel. This underscores the crucial role of HA concentration and crosslinking in determining gel firmness (Sami AlSogair, 2023).

The quadratic model (Table 6, Eq. 2) from our experimental design for Y2: Adhesive force response clearly highlights the significant influence of formulation composition. Specifically, the coefficients of X1: HA% and X2: PUL. As PUL% surpassed the value that of X3: GLY%, it emphasized the pivotal role of HA% and PUL% in impacting adhesive force response (Figure 6). Data obtained from TA, reinforces this relationship, revealing a consistent rise in adhesive force with increasing HA and PUL content (Figures 9-14). The increase in concentration of each polymeric component affecting adhesive force can be attributed to greater polymer entanglement (Andrews et al., 2009).

Y3:Spreadability is a crucial aspect of semisolid formulations, ensuring that formulation evenly distribute when applied to the skin, which in turn enhances patient compliance (Bakhrushina et al., 2022). The software recommended a linear model (Table 6, Eq. 3) for the spreadability response (Y3), which exhibited a strong fit, with p-values well below 0.0001. Notably, X1: HA% (significantly influences the Y3 response, showing a positive correlation between HA% and spreadability. Conversely, X2: PUL% and X3: GLY% exert opposing effects on Y3, as illustrated in Figure 7. An increase in HA concentration resulted in reduced separation time of gel layer in cap from cone probe under a specific load, indicating decreased Y3: Spreadability of the gel, which can also be attributed to the high molecular weight of HA with 1.42 MDa that was used in this study (Sallustio et al., 2023; Sharma et al., 2023).

Y4: Adhesiveness plays a critical role in gels, guaranteeing precise adherence to the target site, thereby optimizing delivery, minimizing waste, improving user experience, and enabling controlled application—a fundamental factor in formulation. The Y4: Adhesiveness response aligns with a quadratic model, showing positive correlations for each parameter (Table 6, Eq. 4; Figure 8). This trend is attributable to the higher overall polymer content, resulting from the joint effect of X1: HA%, X2: PUL%, and X3: GLY%, which enhances polymer chain interactions with surfaces (Jones et al., 2000).

The established guidelines for the optimization procedures, as outlined in Table 4, enabled the establishment of an optimal design scope. The optimal formulation was determined using the "desirability function (d)" approach, which established a design range. This index varies from 0 to 1, with a value approaching 1 signifying the achievement of the experiment's objectives (Pozharani et al., 2023). For verification of experiments, the software produced a total of 100 formulation solutions. Then, five checkpoint formulations were randomly selected from the list of generated solutions, with a desirability value ranging from 0.99 to 1. Additionally, one more formulation (F1) was prepared without PUL for comparison. The selected formulations were subsequently prepared and subjected to experimental evaluation. The acquired data were then compared to the predicted results from the software. The findings demonstrated that the observed values aligned with the predicted values within a 95% confidence interval, affirming the credibility of the model employed in the study (Table 6).

As can be seen from optimal formulations (Table 7), using a constant concentration of HA, which was fixed as 2%, an increase in PUL concentration led to an increase in gel firmness (Figure 5), and conversely decrease in spreadability (Figure 7). It can be seen from Figures 9-14 that as cohesive bonds in the gel system are broken, a less viscous gel results in a more liquid structure by losing its structure, and vice versa. As the TA results show, more force is required to spread a more viscous sample and create a uniform layer of gel on the skin (Lu and Fassihi, 2015).

Information regarding the adhesiveness of the gel can be obtained by lifting the cone probe out of the sample with upward movement. Additionally, the maximum peak on the graph's negative portion, known as the adhesive force value, represents how simple it is to remove the sample from the probe surface. The samples which had a more liquid

texture demonstrated a decrease in adhesiveness as also proved by rheological studies. As can be seen from Table 7 and Fig. 9-14 the more PUL amount in the gels the more adhesiveness and adhesive force required that obtained for the investigated samples (Lu and Fassihi, 2015; Maslii et al., 2020). This characteristic is considered important since PUL and its derivatives are proposed to be used in wound-healing compositions because of their adhesive properties (Ullah et al., 2021).

Furthermore, when the concentration of GLY was decreased to 0.15% from 1%, no significant difference observed between F2 and F6 regarding the investigated properties obtained from TA experiments. Since GLY was incorporated in the gel formulas as moisturizer to increase the hydration of *stratum corneum* (Bogdan et al., 2020).

### 5.2. Further Examination of the Optimized Gel Formulations

#### 5.2.1. pH measurement of the optimized gel formulations

Measured pH values of the tested formulations were optimum for using as a topical formulation matching with the pH of skin and also makes the gel formulations well-suited for dermatological applications, underscoring their reliability and potential skin-friendly attributes (Lukić et al., 2021; Sharma et al., 2023).

#### 5.2.2. Differential scanning calorimetry analysis

DSC studies were conducted for determining the compatibility of the formulation components and for thermal characterization prepared formulations. A crystalline material melts immediately at a temperature and gives a sharp melting point peak. DSC thermogram also give informatioon on the exothermic or endothermic type of reactions, which occcur during the processes of melting and degradation (Dena and El-Sherbiny, 2022). DSC thermograms of the the HA and PUL, physical mixture of HA and PUL as well as gel formulations (F1, F3 and F4) were depicted in Figure 15. The DSC thermogram of pure PUL showed a broad endothermic peak at between 239.69–250.17 °C, which indicated the partly crystalline and amorphous nature of polymer. This result was in concordande with those reported in literature (Singh et al., 2021; Dena and El-Sherbiny, 2022). Also, the wide endothermic peak observed in the thermograms of HA

and PUL as well as HA-PUL physical mixture presented the dehydration process around 80-90 °C (Nikjoo et al., 2021).

An exothermic sharp peak was observed at 239.32 °C for the pure HA, which could be related to with the thermal decomposition of the HA (Pan et al., 2020). The characteristic peaks for HA and PUL were also observed for the HA-PUL physical mixture. This study was also conducted for the gel formulations F1, F2 and F4. The results for gel formulations indicated broad endothermic peaks between 86-100 °C and 121-126 °C, which could be attributed to the loss of water in the formulations that takes place during the heating cycle of the DSC study (Mendonsa et al., 2018; Nikjoo et al., 2021). The characteristic peaks for HA and PUL were also retained for the gel formulations.

### 5.2.3. Rheological evaluation of the optimized gel formulations

The viscosity and flow characteristics of topical formulations have pivotal role in enhancing their performance, stability, and user experience, thereby contributing to the development of highly effective and widely embraced dermatological preparations (Budai et al., 2023). Additionally, understanding the rheological characteristics of gel-based dosage forms is crucial for anticipating their performance under *in vivo* conditions (Bektas et al., 2020; Rençber and Karavana, 2020).

As can be seen from Figures 16-19, the measured viscosity values of all formulations decreased with the increasing shear rate at both 25 and 32 °C. Furthermore, the developed gel formulations exhibited non-Newtonian/pseudoplastic flow at 25 ºC and at 32 °C. Pseudoplastic flow is characterized by a decreased viscosity with the increasing shear rate, indicating shear-thinning behavior of the system. To ensure a gentle application of the gel on the skin, it is essential that the viscosity decreases as the shear rate increases, since this feature was obtained at both 25 ºC (room temperature) and 32 °C indicating a good application and retention on the skin (Binder et al., 2019).

All of the tested formulations, as illustrated in Figure 17 and Figure 19, displayed significant pseudoplastic flow behavior. The inclusion of HA the formulations, which fixed at 2% w/w, resulted in shear thinning during steady-shear flow. This consistent

shear-thinning behavior categorizes all samples as pseudoplastic materials, indicative of a strongly entangled polymer system (Veronica et al., 2019).

The demonstrated flow characteristic holds significant advantages for wound management applications, suggesting the dressings' ability to conform closely to the wound site, ensuring a comfortable fit and uniform coverage. Moreover, the observed thixotropic nature indicates their capacity to maintain structural integrity upon application, thereby fostering an optimal healing environment. The shear-thinning property further enhances ease of application onto the wound bed, promoting uniform coverage without inducing unnecessary trauma (Amoozegar et al., 2022). Furthermore, our rheological studies reveal that high-molecular-weight HA imparts high viscosity and favorable viscoelastic properties to the gel formulations (Rebenda et al., 2020). It is noteworthy that the pronounced increase in shear stress values observed with formulations F3, F4, and F5, could be attributed to the increased PUL concentration from 2 to 8 percent in these formulations as shown in Table 7.

This effect can be more clearly seen with the F4 formulation. In contrast to the anticipated gradual viscosity decrease suggested by Poudel and colleagues for PUL solutions >8% under shear stress, our experiments with formulations containing high-MW HA and increasing PUL percentages showed a distinctive pattern (Poudel et al., 2020). However, it has also been reported that pullulan solutions exhibits non-Newtonian behavior and shear-thinning behavior and PUL solution's shear stress and shear rate graph depict a linear curve (Singh et al., 2023), which was in line with the results obtained in this study. The dynamic oscillatory flow demonstrated the stretching elastic characteristic of the gels, accompanied by a decrease in the cross-over frequency with the increasing concentration of PUL in formulations. The interaction between high-molecular-weight HA and a higher concentration of PUL, leading to an overall increase in polymer content, could play a key role in explaining the subtle changes in texture and flow behavior observed under shear forces.

As can be seen with F1 formulation, which did not contain PUL, resulted in a texture that was notably different from the other formulations, exhibiting a comparatively lower viscosity, in spite of the high molecular mass of HA used in this study, and its fixed concentration in the optimized formulations. This observation demonstrates that the

addition of PUL leads to an increase in viscosity as it is generally used as a thickener, as also shown in the data obtained from TA and rheology experiments in this study (Rai et al., 2021).

### 5.3. *In Vivo* Experiments

Wound healing is complex physiological process which occurs as response to the tissue injury to re-acquirire the integrity of damaged tissue. This process consists of a series of complex interactive phases including hemostasis, inflammation, proliferation, and maturation/remodeling. In the initial phase, platelets initiate hemostasis, with releasing numerous cytokines, hormones, and chemokines to prompt the other stages. The inflammatory cells, particularly neutrophils and macrophages, are attracted by chemokines and cytokines derived from those cells to the wound area. In the inflammatory phase, the influx of inflammatory cells to the wound area plays an important role in wound healing process such as contributing to the release of lysosomal enzymes and reactive oxygen species. In addition, they facilitate the clean-up of various cell debris. Macrophages, which are thought to possess key roles in the wound healing, contribute many events including entanglement of re-epithelialization, granulation tissue formation, angiogenesis, wound cytokine production, and wound contracture. On the other hand, inhibition or elongation of inflammatory stage can result in a improper healing or a chronic wound. Following the inflammatory phase, the proliferation phase occurs, which is responsible for the closure of lesion with simultenaous formation of new connective tissue or granulation tissue and olso for other healing processes, including angiogenesis, fibroplasia, and re-epithelialization. Angiogenesis begins as the vessels begin to bud from the blood vessels surrounding the wound under the influence of vascular endothelial growth factor, and this process develops the blood circulation in the wound area. Thus, nutrients and maintenance of oxygen homeostasis required for wound healing was provided and the process enhances cellular proliferation, tissue regeneration and re-epithelization. Granulation tissue consists of fibroblasts, new budding vessels, and immature collagen (collagen type III). In this phase, some fibroblasts differentiate into myofibroblasts possessing contractile function for bringing wound edges together. In the re-epithelialization, keratinocytes derived from stem cells within the hair follicles and apocrine glands proliferate and influx into the wound. Those cells repopulate the *stratum*

*basale*, and also begin to migrate over the edge of the wound. The re-epithelialization protects the wound from infection and provides desiccation. The remodeling phase begins as the provisional the extracellular matrix and type III collagen is replaced with type I collagen and the remaining cell types of the previous phases undergo apoptosis. In this last stage, the granulation tissue undergoes a gradual remodeling in an effort to restore the normal tissue structure. This results in scar tissue that is less cellular and vascular and shows a progressive increase in the concentration of collagen fibers, giving the wound its final appearance (Gantwerker and Hom, 2012; Gonzalez et al., 2016; Rodrigues et al., 2019).

According to the obtained results from circular excision wound model experiment, when compared to the vehicle, F3 formulation provided a statistically significant reduction in wound area on days 8, 10 and 12, as 51.9%, 59.9% and 91.1%, respectively ($p<0.01$, $p<0.01$, $p<0.0001$, respectively). Also, when compared to the vehicle, the F4 formulation provided a statistically significant reduction in wound area on days 6, 8, 10 and 12 as 54.3%, 62.4%, 87.4% and 97.3% contraction, respectively ($p<0,01$, $p<0.001$, $p<0,001$, $p<0.0001$, respectively). In the reference group (Madecassol®), it was determined that a significant decrease of the contraction was achieved on the 10th and 12th days with rates of 48% and 59.4% ($p<0.05$ and $p<0.01$). (Table 8, Figure 20). These results clearly demonstrate the quick wound healing effect of increasing the concentration of PUL to 8%, the significance of which was observed on day 6 in F4 compared to the other groups. This finding was also consistent with the literature (Priya et al., 2016; Thangavel et al., 2020) .

Furthermore, the histological findings in the present study showed that treatment with F3 formulation provided a better re-epithelization and remarkably reduced inflammatory cells in the granulation tissue (Table 9 and Figure 21). As HA with high MW (1.4 MDa) was used in this study, and also the formulations F1-F4 contained a fixed concentration of HA at 2% (w/w), the anti-inflammatory process could be resulted from the combined effect of HA and PUL. As also indicated in the previous studies, HA with a high MW stimulate anti-inflammatory responses, and can be found during every step of the wound healing process (Dovedytis et al., 2020; Kawano et al., 2021). Furthermore, it

has also been shown that among the externally applied HA with different MWs was found to be highly effective for the treatment of wounds in mice (Kawano et al., 2021).

However, the difference among the formulations on wound healing efficacy could be attributed to the textural and rhelogical behavior of the formulations, with more pronounced effect of PUL as well as its bioactivity that showed a pronounced effect with increased concentration (Figure 20). As slight increases in the existence of fibroblasts, collagenation and neovascularization were observed in F3 group, this clearly demonstrates that it is effective in the anti-inflammatory and wound healing process of the formulations as described earlier. However, in a study by Priya *et al.* 10% PUL hydrogel was formulated without the use of crosslinkers, and their daily topical application of the gel was demonstrated its its ability to cure wounds. The results obtained in this study may be a direct effect of PUL's antioxidant and energy-producing qualities for cells actively involved in healing process like fibroblasts as well as its hygroscopic nature supporting the dehydration of wounds leading to bacterial dehydration to prevent infection, enhanced oxygenation of cells and thus increased wound closure rate resulting in a quick healing process (Priya et al., 2016; Chen et al., 2022; Elangwe et al., 2023). Moreover, it should be noted that the PUL concentrations of %5 and 8% in F3 and F4 produced a pronounced healing effect even much lesser concentrations than hydrogel containing 10% used in previous research as can be clearly seen Figure 20 (Priya et al., 2016). This can be explained by the space filling effect of high molecular weight HA, as large HA molecules have structural regulatory roles and fill up space (Stern et al., 2006). Moreover, the high-water retention capacity of hydrogels makes them potent candidates for wound dressings as they provide a moist environment in the wound and remove excess wound fluid, thereby accelerating wound healing (Elangwe et al., 2023), which can be further enhanced by addition of different bioactive compounds in comparison to standard dry wound dressings (Seiser et al., 2022).

As a conclusion, HA-PUL based gels can be very promising agents in wound-healing process. These results could be mainly attributed to the potential wound healing effect of PUL and partly to the structural regulatory roles and space filling effect of high MW HA used in this study.

# SUMMARY

**ALMATLOB S.K. Investigation of Wound Healing Effect of Hyaluronic Acid/Pullulan Gel Formulations. Van Yüzüncü Yıl University, Institute of Health Sciences, Department of Basic Pharmaceutical Sciences, Master Thesis, Van, 2024.** The wound healing process is initiated after skin damage occurs with external factors such as physical, chemical, thermal, biological and so on. Wound healing normally occurs through well-established, overlapping steps called hemostasis, inflammation, proliferation, and remodeling. However, prolonging the healing process and progression of an acute wound to a chronic wound are undesirable situations that can negatively affect this process, and often cause the development of scar tissue. Various wound care products are available on the market to accelerate and support the wound healing process, targeting both acute and chronic wounds. Although, hydrogels stands out among these products, the requirements of cross-linking natural or synthetic polymers or synthesizing graft copolymers make the development and characterization of this systems more complex. However, gel type formulations can carry advantages of hydrogels in wound healing applications, which can easily be prepared from the physical mixtures of components. This study aimed to develop non-crosslinked gel formulations based on binary physical mixtures of hyaluronic acid and pullulan. A Design of Experiments (DOE) matrix was carried out to reach optimum gel formulations, by using the results obtained by Texture Profile Analysis. After optimizing the gel formulations, the differential scanning calorimetry and rheological studies were performed. After characterizations studies, 4 formulations containing 2% hyaluronic acid and pullulan with various concentrations at 0, 2, 5, and 8% (F1, F2, F3, and F4, respectively) were examined in circular excision wound model in mice. F3 and F4 exhibited more pronunced effect on the investigated wound model compared to the other groups according to the wound area measurements and histopathological study. These results were attributed mainly to the potential wound healing effect of pullulan, and partly to the structural regulatory role and space filling effect hyaluronic acid. This study clearly demonstrate the possible use of pullulan based gels as wound-healing agents.

**Key words:** Hyaluronic acid, pullulan, gel, formulation, wound healing

# GENİŞLETİLMİŞ TÜRKÇE ÖZET

# (EXTENDED SUMMARY IN TURKISH)

## Hyalüronik Asit/Pullulan Jel Formülasyonlarının Yara İyileştirici Etkisinin İncelenmesi

## ÖZET

**ALMATLOB S.K. Hyalüronik Asit/Pullulan Jel Formülasyonlarının Yara İyileştirici Etkisinin İncelenmesi. Van Yüzüncü Yıl Üniversitesi, Temel Eczacılık Bilimleri Anabilim Dalı, Yüksek Lisans Tezi, Van, 2024.** Yara iyileşme süreci fiziksel, kimyasal, termal, biyolojik vb. dış etkenlerle cilt hasarının oluşmasından sonra başlatılır. Yara iyileşmesi normal olarak hemostaz, inflamasyon, proliferasyon ve yeniden şekillenme adı verilen iyi-yapılandırılmış, birbiriyle örtüşen adımlar yoluyla gerçekleşir. Ancak iyileşme sürecinin uzaması ve akut yaranın kronik yaraya ilerlemesi bu süreci olumsuz etkileyebilecek ve sıklıkla skar dokusunun gelişmesine neden olabilecek istenmeyen bir durumdur. Yara iyileşme sürecini hızlandırmak ve desteklemek için hem akut hem de kronik yaraları hedef alan çeşitli yara bakım ürünleri piyasada mevcuttur. Bu ürünler arasında hidrojeller ön plana çıksa da doğal veya sentetik polimerlerin çapraz bağlanması veya graft kopolimerlerinin sentezlenmesi gereklilikleri, bu sistemlerin geliştirilmesini ve karakterizasyonunu daha karmaşık hale getirmektedir. Ancak, jel tipi formülasyonlar bileşenlerin fiziksel karışımlarından basit bir şekilde hazırlanabilirken, aynı zamanda yara uygulamalarında hidrojellerin avantajlarını taşıyabilir. Bu çalışmada, hyalüronik asit ve pullulanın ikili fiziksel karışımı esaslı çapraz bağlı olmayan jel formülasyonlarının geliştirilmesi hedeflendi. Hazırlanan jellerin Tekstür Profil Analizi ile elde edilen sonuçlar kullanılarak optimum formülasyonlara ulaşmak için Deney Tasarımı (DOE) matrisi oluşturuldu. Jel formülasyonlarının optimize edilmesinin ardından diferansiyel taramalı kalorimetri analizi ve reolojik çalışmalar gerçekleştirildi. Daha sonra, %2 hyalüronik asit ve sırasıyla %0, %2, %5 ve %8 olmak üzere çeşitli konsantrasyonlarda pullulan içeren 4 formülasyon (sırasıyla, F1, F2, F3 ve F4) hazırlanarak farelerde dairesel eksizyon yara modelinde incelendi. 12 gün boyunca yapılan yara alanı ölçümünden ve histopatolojik çalışmalardan elde edilen sonuçlara göre F3 ve F4'ün diğer gruplara göre çok daha belirgin *in vivo* etkinlik gösterdiği belirlendi. Bu bulgular esas olarak pullulanın potansiyel yara iyileştirici etkisine ve kısmen de hyalüronik asidin yapısal düzenleyici rolüne ve boşluk doldurma etkisinin bir sonucu olarak yorumlanmaktadır. Bu çalışma, pullulan esaslı jellerin yara iyileştirici formülasyonlar olarak kullanılabileceğini açıkça göstermektedir.

**Anahtar kelimeler:** Hyalüronik asit, pullulan, jel, formülasyon, yara iyileşmesi

# 1. GİRİŞ

İnsan vücudunun en büyük organı olan derinin temel işlevi su açısından zengin iç organları kuru dış ortamdan korumaktır. Sağlıklı bir yaşam için cilt bütünlüğünü korumak ve güçlü bir yara iyileştirme yeteneğine sahip olmak temel ön koşullardır (Shaw ve Martin, 2009; Gonzalez ve ark., 2016).

# 2. GENEL BİLGİLER

## 2.1. Yara İyileşme Süreci

Deri bütünlüğünün ve herhangi bir dokunun zarar görmesi yara olarak tanımlanır. Ayrıca yara bakımının önemi, sağlık sistemleri üzerinde ciddi bir yük oluşturması ve büyük bir zorluk oluşturması nedeniyle de vurgulanabilir. Yarayla ilgili en yüksek harcamaların öncelikle cerrahi yaralar, sonra da diyabetik ayak ülserleri nedeniyle olduğu bildirilmiştir (Almadani ve ark. 2021). Yara iyileşme süreci, cildin bütünlüğünü yeniden sağlamaya yönelik senkronize belirtiler dizisidir. Önemli bir fizyolojik süreç olarak kutanöz yara iyileşmesi, çok sayıda hücre tipinin ve bunların yan ürünlerinin işbirliğini içerir (Shaw ve Martin, 2009; Gonzalez ve ark., 2016). Enflamatuar aşamanın başlarında, lokal bir yaralanmanın neden olduğu lezyonu onarmak için çaba gösterilir. Bu, hücre çoğalması ve posterior farklılaşma sürecinde kollajen birikimi ve yenilenmesiyle oluşturulan özel yapıların yerine kök hücrelerin veya halihazırda mevcut doku hücrelerinin kullanılmasını içerir (Eming ve ark., 2007). Bu aşamalar birbirini karşılıklı olarak dışlamaz; yani bir cilt lezyonunu takiben, yaralanmadan etkilenen hücre tipine bağlı olarak, aynı dokuda yenilenme ve onarım gerçekleşebilir (Şekil 1) (Gonzalez ve ark., 2016).

### 2.1.1. Yara iyileşme sürecini etkileyen faktörler

Yara iyileşme süreci beslenme ve çevresel (Williams ve Barbul, 2003; Arnold ve Barbul, 2006; Almadani ve ark., 2021), radyasyon (Tibbs, 1997; Vignard ve ark., 2013; Almadani ve ark., 2021), sigara (Silverstein, 1992; Sørensen, 2012; Almadani

ve ark., 2021), alkol ve genetik (örn. Cutis laxa (CL), Ehlers-Danlos syndrome) (NIH, 2023) nedenler gibi birçok faktörden etkilenir.

### 2.2. Polisakkaratiler ve Yara İyileştirici Uygulamaları

Polisakkaritler, kiraliteleri, şelasyonları, adsorpsiyon kapasiteleri, güçlü kimyasal reaktiviteleri, işlevsellikleri, biyouyumlulukları, biyolojik olarak parçalanabilmeleri ve toksik olmamaları gibi özelliklerinden dolayı terapötik ajanlar olarak kullanılmaktadır. Hayvan modellerinde ve klinik çalışmalarda yara tedavisinde kullanılan polisakkarit bazlı formülasyonlar genellikle selüloz ve türevleri, aljinatlar, kollajen, kitozan ve türevleri, dekstran, hyalüronik asit, pullulan ve diğerlerini içermektedir. Bunların tümü jellerin, hidrojellerin, yara örtülerinin, filmlerin ve topikal spreylerin geliştirilmesinde tek başına veya kombinasyon halinde kullanılırlar (Ribeiro ve ark., 2019; Cui ve ark., 2022; Elangwe ve ark., 2023). Bu polisakkaritler arasında hyalüronik asit ve pullulan topikal yara iyileştirme uygulamalarında benzersiz özellikleri nedeniyle mevcut çalışmada kullanılmak üzere seçilmiştir.

#### 2.2.1. Hyalüronik asit

Hyalüronik asit (HA) üronik asit ve aminoşekerden oluşan ve tekrarlayan, protein olmayan, β-1,4-D-glukuronik asit ve β-1,3-N-asetilglukozamin birimlerine sahip doğal bir sülfatlanmamış glikozaminoglikan (GAG) molekülüdür (Şekil 2) (Necas ve ark., 2008). Mükemmel viskoelastisite, yüksek su tutma kapasitesi, güçlü biyouyumluluk gibi benzersiz fizikokimyasal özelliklere sahip olması HA'in üstünlükleri arasındadır (Liang ve ark., 2016; Gupta ve ark., 2019).

**Hyalüronik asitin farmakoterapötik etkinliği**

HA sağlıklı biyolojik koşullarda boşlukları doldurmak, vücutta su tutmak, eklemleri kayganlaştırmak ve hücrelerin göçüne izin veren bir matris oluşturmak gibi çeşitli görevleri yerine getirir (Liang ve ark., 2016; Gupta ve ark., 2019).

### Yara iyileşmesinde hyalüronik asit

Hyaluronan, yara iyileşmesinde rol oynayan hücre dışı bir polisakarittir. HA'in yara iyileşme sürecindeki rolü Tablo 3'te özetlenmiştir (Frenkel, 2014).

## 2.2.2. Pullulan

Pullulan (PUL), polimorfik bir mantar olan *Aureobasidium pullulans* tarafından üretilen bir α-D-glukandır (Cheng ve ark., 2011; Li ve ark., 2015; Wei ve ark., 2021). PUL'ın kimyasal yapısı Şekil 3'te gösterilmiştir. Renksiz, kokusuz, toksik olmayan, kanserojen olmayan, son derece biyouyumlu ve biyolojik olarak parçalanabilir özelliklerle karakterize edilen, doğal olarak oluşan bir biyopolimerdir. ABD Gıda ve İlaç Dairesi (FDA) bu biyopolimeri Genel Olarak Güvenli Olarak Tanınan (GRAS) kategorisinde listelemiştir. Farmasötik ve biyomedikal, gıda, kozmetik ve sağlık uygulamaları gibi gelecek vaat eden bir polisakkarittir (de Souza ve ark., 2023; Singh ve ark., 2023).

### Pullulanın yara iyileştirici özellikleri

Doğal olarak oluşan polimerler, hücre dışı matrisin (ECM) özelliklerine benzer özellikleri nedeniyle yara örtülerinin tasarımında ve üretiminde yaygın olarak kullanılır ve sentetik polimerler gibi immünojenik değildir (Mano ve ark., 2007; Frenkel, 2014; Mogoşanu ve Grumezescu, 2014; Graça ve ark., 2020). Sıçanlarda eksizyon yara modelinde, %10 PUL jelinin hücre-uyumlu olduğu ve NIH/3T3 fibroblast hücreleri için toksik olmadığı, povidon-iyot ve kontrol grubuyla karşılaştırıldığında kollajen sentezi ve re-konstrüksiyon yoluyla hızlandırılmış yara iyileşmesi ile hızlı epitelizasyon sağladığı gösterilmiştir (Priya ve ark., 2016; Thangavel ve ark., 2020).

### Hyalüronik asit ve pullulan esaslı yara iyileştirici uygulamaları

HA türevlerinin sentezlenmesi (Fallacara ve ark., 2018), HA-graft-PUL polimerleri (Li ve ark., 2018) ve kolajen-PUL kompozitleri (Wong ve ark., 2011) gibi polisakkaritlerin avantajlarının birleştirilmesiyle daha etkili yara örtülerinin geliştirilmesinde polimer kombinasyonlarının kullanıldığı görülebilir.

## 2.3. Çalışmanın Amacı

Yüksek su tutma kapasiteleri nedeniyle yarayı nemli tutarak ve fazla sıvıyı ortadan kaldırarak yara iyileşmesini destekleyen hidrojeller, yara örtüleri için mükemmel bileşenlerdir (Elangwe ve ark., 2023). Yara örtülerinde sıklıkla kullanılan hidrojeller, doğal veya sentetik polimerlerin çapraz bağlanmasıyla veya graft kopolimerlerinin sentezlenmesiyle işlevselliği arttırılmış malzemeler olarak öne çıkmaktadır Ayrıca, hidrojeller geleneksel kuru yara örtülerine göre daha fazla su tutabilir ve bu da ek biyoaktif bileşikler eklenerek geliştirilebilir. Ancak hidrojellerin geliştirilmesindeki ve karakterizasyonundaki zorluklar fiziksel polimer karışımlarını daha kullanışlı hale getirmektedir (Priya ve ark., 2016; Fallacara ve ark., 2018; Seiser ve ark., 2022).

Bu amaçla HA ve PUL'ın fiziksel karışımlarından hazırlanan jel tipi formülasyonlar yara iyileşme sürecine katkıda bulunabilir ve hızlandırabilir. Literatürde HA ve PUL ikili fiziksel karışımı esaslı çapraz bağlı olmayan jel formülasyonlarının yara iyileştirici etkilerini inceleyen bir çalışmanın bulunmaması bu çalışmanın özgünlüğünü oluşturmaktadır.

# 3. GEREÇ ve YÖNTEM

## 3.1. Gereç

Bu çalışmada kullanılan kimyasallar, sarf malzemeleri ve cihazların listesi Tablo 2 ve Tablo 3'te verilmiştir.

## 3.2. Yöntem

### 3.2.1. Jellerin geliştirilmesinde kullanılan formülasyon yaklaşımı

Deney tasarımı ve tahmin edilen verilerin hesaplanması, Design-Expert 11.0.0 programı (Stat-Ease Inc.; Amerika Birleşik Devletleri) kullanılarak yapıldı. Jel bileşimleri için bu tasarımda bağımsız değişkenler olarak Hyalüronik asit (HA), Pullulan (PUL) ve Gliserol (GLY) oranları seçilirken, jel formülasyonlarının kuvvet (sertlik), yayılabilirlik, adezyon kuvveti ve adeziflik gibi parametreleri ‘’Bağımlı Değişken’’ olarak Tekstür Profil Analizi (TA) deneyleriyle 25°C sıcaklık koşulunda elde edildi. Tablo 4'te Box-Behnken Deney Tasarımı (BBED) matrisinin değişkenleri verilmiştir. Kullanılan program DOE matrisi içerisinde, 12 benzersiz formülasyon ve merkez nokta formülasyonunun 5 kopyası dahil olmak üzere toplam 17 alternatif formülasyon üretti.

### 3.2.2. Jel formülasyonlarının hazırlanması

Jel formülasyonlarını hazırlamak için çeşitli konsantrasyonlardaki HA, 50 ˚C'de çeşitli konsantrasyonlarda GLY içeren bir cam beherdeki distile su içine yavaş yavaş ilave edilerek üstten bir karıştırıcı (HS-100D, Daihan Scientific, Kore) kullanılarak 600 rpm'de karıştırıldı. Homojen bir dispersiyon elde edildikten sonra, çeşitli miktarlarda PUL ilave edildi ve oda sıcaklığına kadar soğutuldu. Daha sonra berrak ve şeffaf bir jel elde edildi (Tuncay Tanrıverdi ve ark., 2018).

### 3.2.3. Tekstür profil analizi

Jel formülasyonlarının TA, bir koni kapak düzeneği ile sıkıştırma modunda bir TA XT plus Tekstür Analiz Cihazı (Stable Microsystems, ABD) kullanılarak incelendi (Bogdan ve ark., 2016; Maslii ve ark., 2020). TA çalışması için kullanılan deney düzeneği Şekil 4'te gösterilmiştir.

### 3.2.4. Veri analizi ve deneysel tasarımın optimizasyon çalışmaları

Design-Expert 11.0.0 programı (Stat-Ease Inc.; Amerika Birleşik Devletleri) kullanılarak yazılımı ile deneysel tasarım incelendi ve her yanıt parametresi için en iyi modeli belirlemeye yardımcı olmak amacıyla polinom denklemleri ve ANOVA analizi kullanarak 3 boyutlu yanıt yüzey grafikleri oluşturuldu (Şekil 5-8).

### 3.2.5. Optimize edilmiş jel formülasyonlarının ileri karakterizasyonu

#### Optimize edilmiş jel formülasyonlarının pH ölçümü

Jellerin pH'ı, cam elektrotlu HANNA HI2202-02 Edge® pH ölçer (Hanna Instruments, ABD) kullanılarak belirlendi. Ölçümler üç tekrar halinde yapıldı ve veriler ortalama ± SS olarak verildi.

#### Diferansiyel taramalı kalorimetri analizi

HA ve PUL'un diferansiyel tarama kalorimetrisi (DSC) analizi, HA ve PUL'un fiziksel karışımı ve jel formülasyonları (F1, F3 ve F4), 100 mL $dk^{-1}$ akış hızı ile 25 °C'den 250 °C'ye 10 °C $dk^{-1}$ ısıtma hızı ile DSC (Setaram Labsys, DSC131 Evo, Fransa) kullanılarak gerçekleştirildi (Mendonsa ve ark., 2018; Pan ve ark., 2020; Singh ve ark., 2021).

#### Optimize edilmiş jel formülasyonlarının reolojik karakterizasyonu

Seçilen altı formülasyon üzerinde reolojik değerlendirmeler gerçekleştirmek için bir TA Discovery HR-1 hibrit reometre (TA Instruments, ABD) kullanıldı. Ölçümler, sıcaklık kontrollü bir Peltier plakası kullanılarak hem 25°C hem de 32°C'de gerçekleştirildi ve 500 μm aralıklı bir çelik Smart Swap TM paralel plaka geometrisi kullanıldı (Bektas ve ark., 2020; Rençber ve Karavana, 2020).

### 3.2.6. *In vivo* deneyler

#### Hayvanlar

Deneylerde Van Yüzüncü Yıl Üniversitesi Deneysel Tıp Uygulama ve Araştırma Merkezi (Van, Türkiye) tarafından sağlanan dişi Swiss fareler (20-25 g) kullanıldı.

Fareler, her grupta 7 hayvan olacak şekilde 7 gruba ayrıldı: Negatif Kontrol, Sıvağ (distile suda GLY, %1, a/a), F1 (HA/GLY, %2/1, a/a), F2 (HA/PUL/GLY, %2/2/1, a/a/a), F3 (HA/PUL/GLY, %2/5/1, a/a/a), F4 (HA/PUL/GLY, %2/8/1, a/a/a) ve Referans (Madecassol®).

**Dairesel eksizyon yara modeli**

Anestezi altındaki farelerde 6 mm çapında biyopsi punch kullanılarak dairesel eksizyon yaraları oluşturuldu ve hayvanlar bölümünde anlatıldığı gibi ajanlar 12 gün boyunca günde bir kez olmak üzere yaralara haricen uygulandı (Sadaf ve ark., 2006). Yaralar dijital kamera (Canon EOS 300D, ABD) ile gün aşırı fotoğraflandı ve yara alanlarının boyutu ImageJ programı kullanılarak hesaplandı (Akkol ve ark., 2011).

**Histolojik prosedürler**

Deri dokularının histopatolojik incelemesi yara iyileşmesi sırasında yara yüzeyinde kabuklanma ve ülser oluşumu, yeniden epitelizasyon (epidermisin rejenerasyonu); dermal inflamatuar hücrelerin infiltrasyonu, fibroblast proliferasyonu, kollajen lif rejenerasyonu ve dermiste neovaskülarizasyon aşağıdaki yarı kantitatif puanlama sistemi kullanılarak belirlendi: yok (-), (+) hafif, (++) orta, (+++) şiddetli (Oz ve ark., 2016).

### 3.2.7. İstatistiksel Analizler

Verilerin normal dağılım gösterip göstermediği Shapiro-Wilk testi ile analiz edildi. Daha sonra Tek yönlü varyans analizi (ANOVA) ve Dunnett post hoc testi yapılarak tüm gruplar sıvağ grubuyla karşılaştırıldı. Ayrıca negatif kontrol grubu, sıvağ grubuyla Student's t testi kullanılarak karşılaştırıldı. İstatistiksel anlamlılık, $p<0,05$ anlamlılık düzeyi ile tüm grupların kontrol grubuyla karşılaştırılması yoluyla belirlendi.

# 4. BULGULAR

## 4.1. Box-Behnken Deney Tasarımının Değerlendirilmesi

Tablo 5, Design Expert 11.0.0 programı (Stat Ease, ABD) kullanılarak Tablo 4'e karşılık gelen BBED matrisi içerisinde oluşturulan değişkenlere, kısıtlamalara ve bunlara karşılık gelen yanıtlara ilişkin 17 formülasyona genel bir bakış sunmaktadır. Ayrıca Tablo 6, BBED Matrix'in uygun modellerinin regresyon denklemlerini göstermektedir. TA çalışmasından elde edilen veriler, Y1, Y2, Y3 ve Y4 sırasıyla sertliği (g), adezyon kuvvetini (g), Y3= yayılabilirliği (g.sn) ve Y4= adezifliği (g.sn) temsil edecek şekilde matrisin geliştirilmesinde kullanıldı.

Şekil 5, 6, 7 ve 8 sırasıyla, bağımsız değişkenler ile sertlik, adezyon kuvveti, yayılabilirlik ve adeziflik cevabı arasındaki ilişkinin 3 boyutlu yüzey grafiğini göstermektedir.

## 4.2. Seçilen Formülasyonlarla Elde Edilen Tekstür Profil Analizi Verileri

Bir koni başlıklı prob kullanılarak F1-6 için TA grafiği elde edilmiştir. Veriler kuvvet (g) ve zaman (saniye) olarak grafik haline getirilmiş ve Şekil 9-14'te gösterilmiştir.

## 4.3. Seçilen formülasyonlarla kullanılan modelin doğrulanması

Box-Behnken Deney Tasarımı kullanılarak yapılan analizler sonucunda, Tablo 7'de sunulan TA çalışmasından elde edilen verilerden de görüldüğü gibi kullanılan modelin validasyonu seçilen formülasyonlar ile gerçekleştirilmiştir.

## 4.4. Optimize edilmiş jel formülasyonlarının ileri karakterizasyonu

### 4.4.1. Optimize edilmiş jel formülasyonlarının pH ölçümü

Altı optimal jel formülasyonunun ölçülen pH değerleri sırasıyla, 6,40 ±0,13, 6,67 ± 0,04, 6,75 ± 0,05, 6,55 ± 0,03, 6,76 ± 0,03 ve 6.69 ± 0,16 olarak bulundu.

### 4.4.2. Diferansiyel taramalı kalorimetri analizi

HA ve PUL, HA ve PUL'un fiziksel karışımı ve jel formülasyonlarının (F1, F3 ve F4) DSC çalışmasından elde edilen termogramları Şekil 15'te verilmiştir.

### 4.4.3. Optimize edilmiş jel formülasyonlarının reolojik değerlendirmesi

Viskozitenin kayma hızının bir fonksiyonu ve kayma gerilimini kayma hızının bir fonksiyonu olarak gösterildiği akış eğrileri Şekil 16-19'da gösterilmiştir.

### 4.4.4. *In vivo* deneyler

**Dairesel eksizyon yara modeli**

Her bir grupta kullanılan ajanların farelerde oluşturulan dairesel eksizyon yara modeli üzerinde 12 gün boyunca gözlemlenen kontraksiyon etkileri Tablo 8'de verilmiştir.

**Histolojik değerlendirmeler**

Farklı deney gruplarına ait yara alanlarından alınan deri dokularındaki histopatolojik lezyonların skorlanması Tablo 9'da özetlenmiştir. Her deney grubu için temsili mikroskobik fotoğraflar Şekil 21'de gösterilmiştir.

# 5. TARTIŞMA VE SONUÇ

## 5.1. Tekstür Profil Analizi Çalışması ve Box-Behnken Deney Tasarımının Değerlendirilmesi

Jeller, doku onarımını kolaylaştıran ve enfeksiyon riskini azaltan nemli, koruyucu bir mikro ortam oluşturarak yara iyileşmesinde kritik bir rol oynar. Ayrıca formülasyonların sertlik, yayılabilirlik, yapışma kuvveti ve adeziflik gibi tekstür özellikleri, formülasyonların akışkanlığını ve deforme edilebilirliğini ortaya koymaktadır (Boateng ve ark., 2008; Maslii ve ark., 2020). Bu özellikler esas alındığında, başarılı bir topikal jel formülasyonunun öncelikli hedefi hızlı yayılma yeteneğidir. Bu, cildin etkili bir şekilde kaplanmasını sağladığından dermatolojik ürünler için özellikle önemlidir. Bu çalışmada da gözlemlendiği gibi, daha akışkan bir kıvama sahip olan numunelerde, reolojik çalışamalardan elde edilen sonuçlardan da görüldüğü gibi sertlikte (Y1 cevabı), adezyon kuvvetinde (Y2 cevabı) ve adeziflikte (Y4 cevabı) azalma gözlemlenmiştir. HA konsantrasyonundaki artış, yayılabilirliğin (Y3 cevabı) yani azaldığını göstermektedir. Bu sonuç, aynı zamanda bu çalışmada kullanılan HA'nın yüksek moleküler ağırlığının (1.42 MDa) da bir sonucu olarak yorumlanabilir (Şekil 5-8). Elde edilen sonuçlar, Design-Expert® programı tarafından oluşturulmuş R2, düzeltilmiş R2, pre-R2 ve p-değeri ($p<0,05$ anlamlılık düzeyinde) dahil olmak üzere istatistiksel parametreler kullanılarak analiz edildi (Tablo 6). Program ile deneylerin doğrulanması için toplam 100 formülasyon çözümü üretildi. Daha sonra, oluşturulan çözümler listesinden arzu edilirlik değeri 0,99 ile 1 arasında değişen beş kontrol noktası formülasyonu rastgele seçildi. Ayrıca karşılaştırma için PUL olmadan bir formülasyon (F1) daha hazırlandı. Optimum formülasyonlardan görülebileceği gibi (Tablo 7), %2 (a/a) olarak sabitlenen bir HA konsantrasyonu kullanıldığında, PUL konsantrasyonundaki bir artış jel sertliğinde artışa ve bunun tersine yayılabilirlikte azalmaya yol açtı. Şekil 9-14'ten, jel sistemindeki bağların kopmasıyla daha az viskozite gösteren bir yapıyla sonuçlanarak akışkanlaşmıştır. TA sonuçlarında görüldüğü gibi, daha viskoz bir numuneyi yaymak ve cilt üzerinde tekdüze bir jel tabakası oluşturmak için daha fazla kuvvet gerekir (Lu ve Fassihi, 2015). Tablo 7 ve Şekil 9-14'ten görülebileceği gibi, incelenen örnekler için jellerdeki PUL miktarı ne kadar fazla olursa, o kadar fazla adezyon kuvveti ve adeziflik elde edilmiştir (Lu ve Fassihi, 2015; Maslii ve ark., 2020). PUL ve türevlerinin adezif özelliklerinden

dolayı yara iyileştirici bileşimlerde kullanılması önerildiğinden bu özelliğin önemli olduğu düşünülmektedir (Ullah ve ark., 2021).

### 5.2. Optimize edilmiş jel formülasyonlarının ileri karakterizasyonu

#### 5.2.1. Optimize edilmiş jel formülasyonlarının pH ölçümü

Optimize edilen formülasyonların ölçülen pH değerleri, cildin pH'ı ile eşleşen topikal bir formülasyon olarak kullanım için optimum düzeyde olup, bu özellik aynı zamanda bu formülasyonları dermatolojik uygulamalar için çok uygun hale getirerek güvenilirliklerinin ve potansiyel cilt dostu özelliklerini göstermektedir (Lukić ve ark., 2021; Sharma ve ark., 2023).

#### 5.2.2. Diferansiyel taramalı kalorimetri analizi

HA ve PUL ve ayrıca HA-PUL fiziksel karışımına ait termogramlarda gözlemlenen endotermik pikler, bu polisakkaritler arasında herhangi bir etkileşim göstermediğini doğrulamıştır. Aynı zamanda, HA ve PUL için karakteristik pikler jel formülasyonları için de korunduğu görülmüştür (Mendonsa ve ark., 2018; Nikjoo ve ark., 2021).

#### 5.2.3. Optimize edilmiş jel formülasyonlarının reolojik karakterizasyonu

Jel tipi dozaj formlarının reolojik özelliklerini anlamak, *in vivo* koşullar altında performanslarını tahmin etmek için çok önemlidir (Bektas ve ark., 2020; Rençber ve Karavana, 2020).

Şekil 16-19'dan görülebileceği gibi, tüm formülasyonların ölçülen viskozite değerleri, hem 25 hem de 32 °C'de artan kesme hızıyla birlikte azalmıştır. Ayrıca geliştirilen jel formülasyonları 25 °C ve 32 °C'de Newtonian olmayan/psödoplastik akış sergilemiştir. Psödoplastik akış, sistemin kayma incelmesi davranışını gösteren, artan kayma hızıyla birlikte azalan viskozite ile karakterize edilir. Jelin cilt üzerinde hassas bir şekilde uygulanmasını sağlamak için, kayma hızının artmasıyla viskozitenin azalması önemlidir, çünkü bu özellik hem 25 °C'de (oda sıcaklığı) hem de 32 °C'de elde edilerek cilt üzerinde uygulama kolaylığı ve tutulma anlamına gelmektedir (Binder ve ark., 2019). Formülasyonlarda HA'in %2 (a/a) konsantrasyonuna sabitlenmesi psödoplastik davranışı

gösteren sabit kayma akışı sırasında kayma incelmesiyle sonuçlanmıştır (Şekil 17 ve Şekil 19). Bu özellik, güçlü bir şekilde dolanıklık sergileyen bir polimer sisteminin göstergesidir (Veronica ve ark., 2019). Sergilenen akış karakteristiği, yara iyileştiricilerin uygulanması için önemli avantajlara sahiptir. Örneğin, yara örtülerinin yara bölgesine tam uyum sağlaması, eşit bir kaplama sağlama yeteneğini ortaya koyar (Amoozegar ve ark., 2022).

### 5.3. *In Vivo* Deneyler

Dairesel eksizyon yara modeli deneyinden elde edilen sonuçlara göre, F3 formülasyonu sıvağ ile karşılaştırıldığında yara alanında 8., 10. ve 12. günlerde sırasıyla, %51,9, %59,9 ve %91,1 olmak üzere istatistiksel olarak anlamlı bir azalma sağladı (sırasıyla, $p<0,01$, $p<0,01$, $p<0,0001$). Ayrıca F4 formülasyonu sıvağ ile karşılaştırıldığında yara alanında 6., 8., 10. ve 12. günlerde sırasıyla, %54,3, %62,4, %87,4 ve %97,3 olmak üzere istatistiksel olarak anlamlı bir azalma sağladı (sırasıyla, $p<0,01$, $p<0,001$, $p<0,001$, $p<0,0001$). Referans grubunda (Madecassol®) 10. ve 12. günlerde %48 ve %59,4 kontraksiyon oranları ile yara alanında anlamlı bir azalma sağlandığı belirlendi ($p<0,05$ ve $p<0,01$) (Tablo 8, Şekil 20). Bu sonuçlar, F4 grubunda diğer gruplarla karşılaştırıldığında 6. günde hızlı yara iyileştirme etkisi üzerinde PUL konsantrasyonunun %8'e çıkarılmasının önemini açıkça göstermektedir. Bu sonucun literatürle de uyumlu olduğu görülmektedir (Priya ve ark., 2016; Thangavel ve ark., 2020).

Mevcut çalışmadaki histolojik bulgular, F3 formülasyonunun, daha iyi bir re-epitelizasyon sağladığı ve granülasyon dokusundaki inflamatuar hücreleri belirgin şekilde azalttığını göstermiştir (Tablo 9, Şekil 21). Bu çalışmada yüksek molekül ağırlıklı HA (1,4 MDa) kullanıldığından ve ayrıca F1-F4 formülasyonları %2 (a/a) sabit HA konsantrasyonu içerdiğinden, anti-inflamatuar sürecin HA-PUL kombinasyon etkisinden kaynaklanabileceği düşünülmektedir. Önceki çalışmalarda da belirtildiği gibi, daha yüksek molekül ağırlıklı HA, anti-inflamatuar yanıtı uyarmaktadır ve yara iyileşme sürecinin her aşamasında rol oynayabilir (Dovedytis ve ark., 2020; Kawano ve ark., 2021). Ayrıca, haricen uygulanan farklı molekül ağırlığına sahip HA'ların farelerde yara iyileştirmede oldukça etkili olduğu da gösterilmiştir (Kawano ve ark., 2021). Bununla birlikte, yara iyileştirme etkinliği konusunda formülasyonlar arasındaki fark,

formülasyonların tekstürel ve reolojik davranışı olarak yorumlanabilir. Bu çalışmada PUL'ın artan konsantrasyonuyla birlikte daha belirgin etki gösterdiği belirlenmiştir (Şekil 20).

Sonuç olarak HA-PUL esaslı jeller yara iyileşme sürecinde umut verici formülasyonlar olarak görülmektedir. Bu sonuçlar esas olarak PUL'ın potansiyel yara iyileştirici etkisinin ve kısmen de bu çalışmada kullanılan yüksek molekül ağırlıklı HA'in yapısal düzenleyici rolünün ve boşluk doldurucu etkisinin bir sonucu olarak yorumlanabilir.

## REFERENCES


Ahmed N. Advanced glycation endproducts—role in pathology of diabetic complications. Diabetes Res Clin Pract. 2005;67(1):3-21.

Akkol EK, Süntar I, Keles H, Yesilada E. The potential role of female flowers inflorescence of Typha domingensis Pers. in wound management. J Ethnopharmacol. 2011;133(3):1027-32.

Almadani YH, Vorstenbosch J, Davison PG, Murphy AM, (Eds). Wound healing: A comprehensive review. Seminars in Plastic Surgery; 2021: Thieme Medical Publishers, Inc. 333 Seventh Avenue, 18th Floor, New York, NY.

Alon R, Nourshargh S. Learning in motion: Pericytes instruct migrating innate leukocytes. Nat Immunol. 2013;14(1):14-5.

Amoozegar H, Ghaffari A, Keramati M, Ahmadi S, Dizaji S, Moayer F, et al. A novel formulation of simvastatin nanoemulsion gel for infected wound therapy: In vitro and in vivo assessment. J Drug Deliv Sci. 2022;72:103369.

Andrews GP, Laverty TP, Jones DS. Mucoadhesive polymeric platforms for controlled drug delivery. Eur J Pharm Biopharm. 2009;71(3):505-18.

Arnold M, Barbul A. Nutrition and wound healing. Plast Reconstr Surg. 2006;117(7S):42S-58S.

Autissier A, Letourneur D, Le Visage C. Pullulan-based hydrogel for smooth muscle cell culture. J Biomed Mater Res A 2007;82(2):336-42.

Bakhrushina E, Anurova M, Zavalniy M, Demina N, Bardakov A, Krasnyuk I. Dermatologic gels spreadability measuring methods comparative study. Int J Appl Pharm. 2022;14(1):164-8.

Bektas N, Şenel B, Yenilmez E, Özatik O, Arslan R. Evaluation of wound healing effect of chitosan-based gel formulation containing vitexin. Saudi Pharm J. 2020;28(1):87-94.

Binder L, Mazál J, Petz R, Klang V, Valenta C. The role of viscosity on skin penetration from cellulose ether-based hydrogels. Skin Res Technol. 2019;25(5):725-34.

Boateng JS, Matthews KH, Stevens HN, Eccleston GM. Wound healing dressings and drug delivery systems: a review. J Pharm Sci. 2008;97(8):2892-923.

Bogdan C, Moldovan ML, Man IM, Crișan M. Preliminary study on the development of an antistretch marks water-in-oil cream: ultrasound assessment, texture analysis, and sensory analysis. Clin Cosmet Investig Dermatol. 2016:249-55.

Borzacchiello A, Russo L, Malle BM, Schwach-Abdellaoui K, Ambrosio L. Hyaluronic acid based hydrogels for regenerative medicine applications. Biomed Res Int. 2015;2015.

Budai L, Budai M, Fülöpné Pápay ZE, Vilimi Z, Antal I. Rheological Considerations of Pharmaceutical Formulations: Focus on Viscoelasticity. Gels. 2023;9(6):469.

Calin MA, Coman T, Calin MR. The effect of low level laser therapy on surgical wound healing. Rom Rep Phys. 2010;62(3):617-27.

Callewaert B, Malfait F, Loeys B, De Paepe A. Ehlers-Danlos syndromes and Marfan syndrome. Best Pract Res Clin Rheumatol 2008;22(1):165-89.

Carmeliet P. Angiogenesis in health and disease. Nat Med. 2003;9(6):653-60.

Chen K, Sivaraj D, Davitt MF, Leeolou MC, Henn D, Steele SR, et al. Pullulan-Collagen hydrogel wound dressing promotes dermal remodelling and wound healing compared to commercially available collagen dressings. Wound Repair Regen. 2022;30(3):397-408.

Chen WJ. Functions of hyaluronan in wound repair. Wound Repair Regen. 2002;2:147-56.

Chen WY, Marcellin E, Hung J, Nielsen LK. Hyaluronan molecular weight is controlled by UDP-N-acetylglucosamine concentration in Streptococcus zooepidemicus. J Biol Chem 2009;284(27):18007-14.

Cheng K-C, Demirci A, Catchmark JM. Pullulan: biosynthesis, production, and applications. Appl Microbiol Biotechnol. 2011;92:29-44.

Choi SS, Diehl AM. Epithelial-to-mesenchymal transitions in the liver. J Hepatol. 2009;50(6):2007-13.

Chong HC, Tan MJ, Philippe V, Tan SH, Tan CK, Ku CW, et al. Regulation of epithelial–mesenchymal IL-1 signaling by PPARβ/δ is essential for skin homeostasis and wound healing. J Cell Biol 2009;184(6):817-31.

Cui R, Zhang L, Ou R, Xu Y, Xu L, Zhan X-Y, et al. Polysaccharide-based hydrogels for wound dressing: Design considerations and clinical applications. Front Bioeng. 2022;10:845735.

de Souza CK, Ghosh T, Lukhmana N, Tahiliani S, Priyadarshi R, Hoffmann TG, et al. Pullulan as a sustainable biopolymer for versatile applications: A review. Mater Today Commun. 2023:106477.

Decker MR, Greenblatt DY, Havlena J, Wilke LG, Greenberg CC, Neuman HB. Impact of neoadjuvant chemotherapy on wound complications after breast surgery. Surgery 2012;152(3):382-8.

Dena ASA, El-Sherbiny IM. Biological macromolecules for nucleic acid delivery. Biological Macromolecules: Elsevier; 2022. p. 479-90.

Deptuła M, Zieliński J, Wardowska A, Pikuła M. Wound healing complications in oncological patients: perspectives for cellular therapy. Postepy Dermatol Alergol. 2019;36(2):139-46.

Dovedytis M, Liu ZJ, Bartlett S. Hyaluronic acid and its biomedical applications: A review. Eng Regen. 2020;1:102-13.

Elangwe CN, Morozkina SN, Olekhnovich RO, Polyakova VO, Krasichkov A, Yablonskiy PK, et al. Pullulan-based hydrogels in wound healing and skin tissue engineering applications: A review. Int J Mol Sci. 2023;24(5):4962.

Eming SA, Krieg T, Davidson JM. Inflammation in wound repair: molecular and cellular mechanisms. J Investig Dermatol. 2007;127(3):514-25.

Fallacara A, Baldini E, Manfredini S, Vertuani S. Hyaluronic acid in the third millennium. J Polym. 2018;10(7):701.

Fallacara A, Vertuani S, Panozzo G, Pecorelli A, Valacchi G, Manfredini S. Novel artificial tears containing cross-linked hyaluronic acid: an in vitro re-epithelialization study. Molecules. 2017;22(12):2104.

Firlar I, Altunbek M, McCarthy C, Ramalingam M, Camci-Unal G. Functional hydrogels for treatment of chronic wounds. Gels. 2022;8(2):127.

Frenkel JS. The role of hyaluronan in wound healing. Int Wound J. 2014;11(2):159-63.

Gantwerker EA, Hom DB. Skin: histology and physiology of wound healing. Clin Plast Surg. 2012;39(1):85-97.

Garg RK, Auerbach LJ, Sorkin M, Rennert RC, Longaker MT, Gurtner GC. A biomimetic collagen-pullulan hydrogel enhances stemness and wound healing potential of adipose-derived mesenchymal stem cells. J Am Coll Surg. 2012;215(3):S96.

Gonzalez ACO, Costa TF, Andrade ZdA, Medrado ARAP. Wound healing-A literature review. An Bras Dermatol. 2016;91:614-20.

Graça MF, Miguel SP, Cabral CS, Correia IJ. Hyaluronic acid—Based wound dressings: A review. Carbohydr Polym. 2020;241:116364.

Guo Sa, DiPietro LA. Factors affecting wound healing. J Dent Res. 2010;89(3):219-29.

Gupta RC, Lall R, Srivastava A, Sinha A. Hyaluronic acid: molecular mechanisms and therapeutic trajectory. Front Vet Sci. 2019;6:192.

Gurtner GC, Werner S, Barrandon Y, Longaker MT. Wound repair and regeneration. Nature. 2008;453(7193):314-21.

Jones DS, Woolfson AD, Brown AF, Coulter WA, McClelland C, Irwin CR. Design, characterisation and preliminary clinical evaluation of a novel mucoadhesive topical formulation containing tetracycline for the treatment of periodontal disease. J Control Release. 2000;67(2-3):357-68.

Jung MK, Callaci JJ, Lauing KL, Otis JS, Radek KA, Jones MK, et al. Alcohol exposure and mechanisms of tissue injury and repair. Alcohol Clin Exp Res. 2011;35(3):392-9.

Kawano Y, Patrulea V, Sublet E, Borchard G, Iyoda T, Kageyama R, et al. Wound healing promotion by hyaluronic acid: Effect of molecular weight on gene expression and in vivo wound closure. Pharm. 2021;14(4):301.

Kumar V., Abbas AK., Aster JC. Robbins & Cotran Pathologic Basis of Disease, 10th Edition. Elsevier; 2020.

Landén NX, Li D, Ståhle M. Transition from inflammation to proliferation: a critical step during wound healing. Cell Mol Life Sci. 2016;73:3861-85.

Li H, Xue Y, Jia B, Bai Y, Zuo Y, Wang S, et al. The preparation of hyaluronic acid grafted pullulan polymers and their use in the formation of novel biocompatible wound healing film. Carbohydr Polym. 2018;188:92-100.

Li J, Chen J, Kirsner R. Pathophysiology of acute wound healing. Clin Dermatol. 2007;25(1):9-18.

Li Y, Chi Z, Wang G-Y, Wang Z-P, Liu G-L, Lee C-F, et al. Taxonomy of Aureobasidium spp. and biosynthesis and regulation of their extracellular polymers. Crit Rev Microbiol. 2015;41(2):228-37.

Liang J, Jiang D, Noble PW. Hyaluronan as a therapeutic target in human diseases. Adv Drug Deliv Rev. 2016;97:186-203.

Lu Z, Fassihi R. Influence of colloidal silicon dioxide on gel strength, robustness, and adhesive properties of diclofenac gel formulation for topical application. AAPS PharmSciTech. 2015;16:636-44.

Lukić M, Pantelić I, Savić SD. Towards optimal pH of the skin and topical formulations: From the current state of the art to tailored products. Cosmetics. 2021;8(3):69.

Mano J, Silva G, Azevedo HS, Malafaya P, Sousa R, Silva SS, et al. Natural origin biodegradable systems in tissue engineering and regenerative medicine: present status and some moving trends. J R Soc Interface. 2007;4(17):999-1030.

Martin P. Wound healing--aiming for perfect skin regeneration. J Cell Sci. 1997;276(5309):75-81.

Maslii Y, Ruban O, Kasparaviciene G, Kalveniene Z, Materiienko A, Ivanauskas L, et al. The influence of pH values on the rheological, textural and release properties of Carbomer Polacril® 40P-based dental gel formulation with plant-derived and synthetic active components. Molecules. 2020;25(21):5018.

Mason DE, Mitchell KE, Li Y, Finley MR, Freeman LC. Molecular basis of voltage-dependent potassium currents in porcine granulosa cells. Mol Pharmacol. 2002;61(1):201-13.

Medrado AR, Pugliese LS, Reis SRA, Andrade ZA. Influence of low level laser therapy on wound healing and its biological action upon myofibroblasts. Lasers Surg Med. 2003;32(3):239-44.

Mendonsa NS, Murthy SN, Hashemnejad SM, Kundu S, Zhang F, Repka MA. Development of poloxamer gel formulations via hot-melt extrusion technology. Int J Pharm. 2018;537(1-2):122-31.

Mogoşanu GD, Grumezescu AM. Natural and synthetic polymers for wounds and burns dressing. Int J Pharm. 2014;463(2):127-36.

Morava E, Guillard M, Lefeber DJ, Wevers RA. Autosomal recessive cutis laxa syndrome revisited. Eur J Hum Genet. 2009;17(9):1099-110.

Nayak BS, Sandiford S, Maxwell A. Evaluation of the wound-healing activity of ethanolic extract of Morinda citrifolia L. leaf. J Evid Based Complementary Altern Med. 2009;6:351-6.

Necas J, Bartosikova L, Brauner P, Kolar J. Hyaluronic acid (hyaluronan): a review. J Vet Med. 2008;53(8):397-411.

National Institutes of Health (NIH). Poor wound healing [Internet]. 2023 [Access date: 10/06/2023]. Available from: https://www.ncbi.nlm.nih.gov/medgen/377525.

Nikjoo D, van der Zwaan I, Brülls M, Tehler U, Frenning G. Hyaluronic acid hydrogels for controlled pulmonary drug delivery—a particle engineering approach. Pharmaceutics. 2021;13(11):1878.

Nunes PS, Albuquerque-Junior RL, Cavalcante DR, Dantas MD, Cardoso JC, Bezerra MS, et al. Collagen-based films containing liposome-loaded usnic acid as dressing for dermal burn healing. Biomed Res Int. 2011;2011.

Oz B, Ilhan M, Ozbilgin S, Akkol E, Acikara O, Saltan G, et al. Effects of Alchemilla mollis and Alchemilla persica on the wound healing process. Bangladesh J Pharmacol. 2016;11(3).

Pan NC, Bersaneti GT, Mali S, Celligoi MAPC. Films based on blends of polyvinyl alcohol and microbial hyaluronic acid. Bangladesh J Pharmacol. 2020;63.

Poudel D, Swilley-Sanchez S, O'keefe S, Matson J, Long T, Fernández-Fraguas CJP. Novel electrospun pullulan fibers incorporating hydroxypropyl-β-cyclodextrin: morphology and relation with rheological properties. Polymers. 2020;12(11):2558.

Pozharani LB, Baloglu E, Suer K, Guler E, Burgaz EV, Kunter I. Development and optimization of in-situ gels for vaginal delivery of metronidazole and curcumin via box-behnken design: In vitro characterization and anti-trichomonas activity. J Drug Deliv Sci Technol. 2023;86:104739.

Priya VS, Iyappan K, Gayathri V, William S, Suguna L. Influence of pullulan hydrogel on sutureless wound healing in rats. Wound Med. 2016;14:1-5.

Qing CJCJoT. The molecular biology in wound healing & non-healing wound. Chin J Traumatol. 2017;20(04):189-93.

Rai M, Wypij M, Ingle AP, Trzcińska-Wencel J, Golińska P. Emerging trends in pullulan-based antimicrobial systems for various applications. Int J Mol Sci. 2021;22(24):13596.

Rebenda D, Vrbka M, Čípek P, Toropitsyn E, Nečas D, Pravda M, et al. On the dependence of rheology of hyaluronic acid solutions and frictional behavior of articular cartilage. Materials. 2020;13(11):2659.

Rençber S, Karavana SY. Formulation and optimization of gellan gum-poloxamer based dexamethasone mucoadhesive in situ gel. J Pharm Res. 2020;24(4):529-38.

Ribatti D, Nico B, Crivellato E. The role of pericytes in angiogenesis. Int J Dev Biol. 2011;55(3):261-8.

Ribeiro D, Carvalho Júnior A, Vale de Macedo G, Chagas V, Silva L, Cutrim B, et al. Polysaccharide-Based Formulations for Healing of Skin-Related Wound Infections: Lessons from Animal Models and Clinical Trials. Biomolecules. 2019;10(1):63.

Ribeiro DML, Carvalho Junior AR, Vale de Macedo GHR, Chagas VL, Silva LdS, Cutrim BdS, et al. Polysaccharide-based formulations for healing of skin-related wound infections: lessons from animal models and clinical trials. Biomolecules. 2019;10 (1):63.

Rodrigues M, Kosaric N, Bonham CA, Gurtner GC. Wound healing: a cellular perspective. Physiol Rev. 2019;99(1):665-706.

Rosen BP. Biochemistry of arsenic detoxification. FEBS Lett. 2002;529(1):86-92.

Ruiter D, Schlingemann R, Westphal J, Denijn M, Rietveld F, De Waal RM. Angiogenesis in wound healing and tumor metastasis. Behring Inst Mitt. 1993(92):258-72.

Rustad KC, Wong VW, Sorkin M, Glotzbach JP, Major MR, Rajadas J, et al. Enhancement of mesenchymal stem cell angiogenic capacity and stemness by a biomimetic hydrogel scaffold. J Biomaterials. 2012;33(1):80-90.

Sadaf F, Saleem R, Ahmed M, Ahmad SI. Healing potential of cream containing extract of Sphaeranthus indicus on dermal wounds in Guinea pigs. J Ethnopharmacol. 2006;107(2):161-3.

Sallustio V, Farruggia G, Di Cagno MP, Tzanova MM, Marto J, Ribeiro H, et al. Design and Characterization of an Ethosomal Gel Encapsulating Rosehip Extract. Gels. 2023;9(5):362.

Sami AlSogair S. Rheology of Hyaluronic Acid Dermal Fillers: Understanding the Science to Improve Results in Clinical Practice. Int J Med Health Res. 2023;2(5):96-103.

Schwartzfarb EM, Romanelli P. Hyperhomocysteinemia and lower extremity wounds. Int J Low Extrem Wounds. 2008;7(3):126-36.

Seiser S, Cerbu D, Gallhofer A, Matiasek J, Elbe-Bürger AJSR. Comparative assessment of commercially available wound gels in ex vivo human skin reveals major differences in immune response-modulatory effects. Sci Rep. 2022;12(1):17481.

Sharma T, Thakur S, Kaur M, Singh A, Jain SK. Novel Hyaluronic Acid ethosomes based gel formulation for topical use with reduced toxicity, better skin permeation, deposition, and improved pharmacodynamics. J Liposome Res. 2023;33(2):129-43.

Shaw TJ, Martin P. Wound repair at a glance. J Cell Sci. 2009;122(18):3209-13.

Sicklick JK, Li Y-X, Jayaraman A, Kannangai R, Qi Y, Vivekanandan P, et al. Dysregulation of the Hedgehog pathway in human hepatocarcinogenesis. J Carcinog. 2006;27(4):748-57.

Silverstein P. Smoking and wound healing. Am J Med. 1992;93(1):S22-S4.

Singh RS, Kaur N, Singh D, Purewal SS, Kennedy JF. Pullulan in pharmaceutical and cosmeceutical formulations: A review. Int J Biol Macromol. 2023;231:123353.

Singh RS, Saini GK, Kennedy JF. Pullulan production in stirred tank reactor by a colour-variant strain of Aureobasidium pullulans FB-1. Carbohydr Polym. 2021;2:100086.

Sørensen LT. Wound healing and infection in surgery: the pathophysiological impact of smoking, smoking cessation, and nicotine replacement therapy: a systematic review. Ann Surg. 2012;255(6):1069-79.

Stern R, Asari AA, Sugahara KN. Hyaluronan fragments: an information-rich system. Eur J Cell Biol. 2006;85(8):699-715.

Su W-H, Cheng M-H, Lee W-L, Tsou T-S, Chang W-H, Chen C-S, et al. Nonsteroidal anti-inflammatory drugs for wounds: pain relief or excessive scar formation? Mediators Inflamm 2010;2010.

Sugahara K, Schwartz N, Dorfman A. Biosynthesis of hyaluronic acid by Streptococcus. J Biol Chem. 1979;254(14):6252-61.

Thangavel P, Vilvanathan SP, Kuttalam I, Lonchin S. Topical administration of pullulan gel accelerates skin tissue regeneration by enhancing collagen synthesis and wound contraction in rats. Int J Biol Macromol. 2020;149:395-403.

Tibbs MK. Wound healing following radiation therapy: a review. J Radiat Oncol. 1997;42(2):99-106.

Tidball JG. Inflammatory processes in muscle injury and repair. Am J Physiol Regul Integr Comp Physiol. 2005;288(2):R345-R53.

Tønnesen H, Pedersen S, Lavrsen M, Tuxøe JI, Thomsen CF. Reduced wound healing capacity in alcohol abusers–reversibility after withdrawal. J Clin Health Promot. 2012;2(3):89-92.

Tonnesen MG, Feng X, Clark RA, (Eds). Angiogenesis in wound healing. J Investig Dermatol Symp Proc; 2000: Elsevier.

Tudu M, Samanta A. Natural polysaccharides: Chemical properties and application in pharmaceutical formulations. Eur Polym J. 2022;184:111801.

Tuncay Tanrıverdi S, Cheaburu-Yilmaz CN, Carbone S, Özer Ö. Preparation and in vitro evaluation of melatonin-loaded HA/PVA gel formulations. Pharm Dev Technol. 2018;23(8):815-25.

Ullah MW, Ul-Islam M, Khan T, Park JK. Recent developments in the synthesis, properties, and applications of various microbial polysaccharides. Handbook of Hydrocolloids. 2021:975-1015.

Veronica M, Fabio G, Nicola V, Paolo P, Enrica B. Differences among Three Branded Formulations of Hyaluronic Acid: Data from Environmental Scanning Electron Microscope Profile, Rheology Behavior and Biological Activity. Biomed J Sci Tech Res. 2019;17(1):12468-78.

Vignard J, Mirey G, Salles B. Ionizing-radiation induced DNA double-strand breaks: a direct and indirect lighting up. Radiother Oncol. 2013;108(3):362-9.

Wang AS, Armstrong EJ, Armstrong AW. Corticosteroids and wound healing: clinical considerations in the perioperative period. Am J Surg. 2013;206(3):410-7.

Wei X, Liu G-L, Jia S-L, Chi Z, Hu Z, Chi Z-M. Pullulan biosynthesis and its regulation in Aureobasidium spp. Carbohydr Polym. 2021;251:117076.

Wicke C, Halliday B, Allen D, Roche NS, Scheuenstuhl H, Spencer MM, et al. Effects of steroids and retinoids on wound healing. Arch Surg. 2000;135(11):1265-70.

Williams JZ, Barbul A. Nutrition and wound healing. Surgical Clinics. 2003;83(3):571-96.

Wong VW, Rustad KC, Galvez MG, Neofytou E, Glotzbach JP, Januszyk M, et al. Engineered pullulan–collagen composite dermal hydrogels improve early cutaneous wound healing. Tissue Eng Part A. 2011;17(5-6):631-44.

Zeisberg M, Neilson EG. Biomarkers for epithelial-mesenchymal transitions. J Clin Investig. 2009;119(6):1429-37.

**RESUME**

# APPENDIX